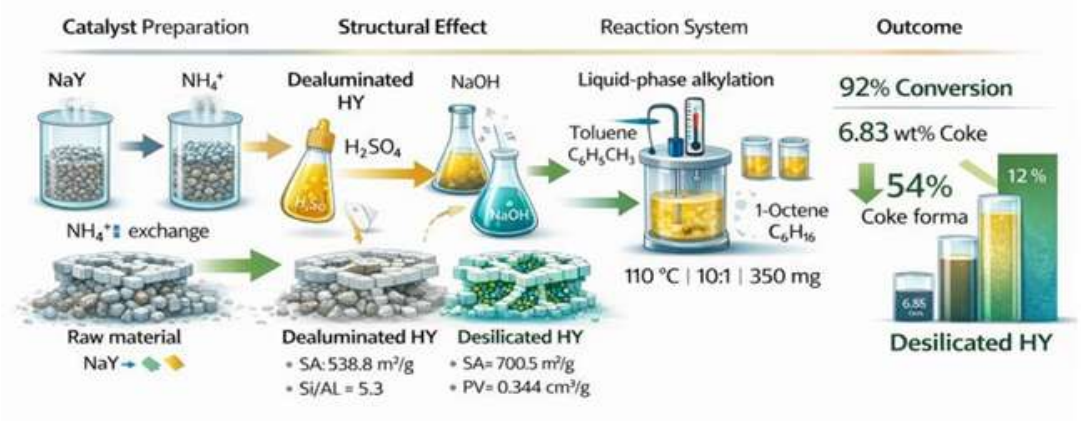
# *Hierarchical Mesoporosity Surpasses Acidity Reduction For Mitigating Coke Deactivation: Comparative Study Of Desilicated And Dealuminated HY Zeolites In Aromatic Alkylation*

Alhumam A. Al-Shammari [a], Bashir Y. Al-Zaidi [a], Ali Al-Shathr [b,*]

[a] Department of Chemical Process Engineering, College of Chemical Engineering, University of Technology- Iraq, Baghdad 10066, Iraq
[b] Department of Petroleum Refining and Gas Technology Engineering, College of Chemical Engineering, University of Technology- Iraq, Baghdad 10066, Iraq
che.22.16@grad.uotechnology.edu.iq; bashir.y.sherhan@uotechnology.edu.iq
* Correspondence: ali.r.mohammedjawad@uotechnology.edu.iq

***Abstract***
Liquid-phase aromatic alkylation over HY zeolites offers an efficient route to alkylated aromatics. Secondary oligomerization and polyalkylation during reaction generate heavy hydrocarbon species that accumulate as coke within the pore network and on Brønsted acid sites, reduce site accessibility, and shorten time-on-stream stability. Post-synthesis modification that tunes acidity or introduces hierarchical porosity remains necessary to lessen deactivation and improve catalytic durability. The study examines freshly prepared HY alongside dealuminated and desilicated HY in liquid-phase alkylation of toluene with 1-octene, with a focus on catalytic activity, stability, and coke deposition behavior. Hydrothermal synthesis of Na-Y was used to prepare the parent HY zeolite, which was then subjected to double ammonium ion exchange and activated by heating. Desilicated HY showed enhanced crystallinity and a high specific surface area (700.5 $m^2$ $g^{-1}$) and maintained the total pore volume (0.344 $cm^3$ $g^{-1}$), with the microporous FAU framework largely intact. Dealuminated HY, in contrast, exhibited partial framework degradation, a decreased surface area (538.8 $m^2$ $g^{-1}$), and a higher Si/Al ratio of 5.3 .
Optimized testing in a batch reactor (toluene:1-octene molar ratio of 10:1, 110 °C, and 350 mg catalyst) showed that desilicated HY achieved the highest 1-octene conversion (92%) and maintained high stability over 300 min on stream. Post-reaction TGA and CHNS results indicated that desilicated HY contained the lowest coke content (6.83 wt.%), a decrease of about 54% compared with fresh HY (12.62 wt.%). Enhanced diffusion of bulky intermediates through hierarchical mesopores inhibited secondary polymerization and reduced the formation of hard coke. The findings indicate that controlled desilication is more effective in reducing catalyst deactivation in alkylation reactions involving bulky intermediates than acidity reduction through dealumination.
**Keywords:** HY zeolite, post-synthesis modification, dealumination, desilication, hierarchical zeolite.

## *Graphical Abstract*



## *1. Introduction*

This aromatic hydrocarbon alkylation reaction with olefins is a key reaction in the petrochemical business, and it allows the generation of the high-value intermediates that are employed in the surfactants, detergents, lubricants, and specialty chemicals [1]. In these, the alkylation of toluene with linear olefins, including 1-octene, has received a lot of attention, whereby the resultant octyl-toluene isomers, especially 2-octyltoluene, are the major building blocks in the bulk and fine chemicals sectors [2]. Traditional Friedel-Crafts alkylation has long been based on homogeneous Lewis acid catalysts, such as $AlCl_3$ and HF [3]. Although they are highly active, these systems are characterized by serious environmental and safety issues, a complicated downstream separation, corrosivity, and low recyclability of catalysts, which drives the shift to the heterogeneous catalysts that are environmentally benign [4].

Solid acids based on zeolites, in particular, protonated Y-type zeolites (HY, FAU framework) have become some of the most effective substitutes for aromatic alkylation reactions [5]. Their highly uniform microporous topology, thermal stability and adjustable Brønsted acidity allow reaction pathways, level of conversion and content to be controlled with high selectivity [6, 7]. The supercage arrangement of HY zeolite which has a pore opening of around 7.4 Å offers a good condition in the formation of carbocation and subsequent electrophilic substitution on aromatic rings [8]. At the same time, the pore geometry of confinement provides steric effects that inhibit polyalkylation and favor selective mono-alkylation, usually leading to ortho-substituted products.

Irrespective of these benefits, the use of zeolite catalysts in the industrial setting is often curtailed due to quick deactivation of the zeolites through the development of carbonaceous deposits, otherwise known as coke [9]. The coke formation is a natural result of reactions of hydrocarbons on the basis of acidic zeolites and is the result of condensing, oligomerizing, and polymerizing the reactive intermediates that are trapped in the microporous network [10]. With bulky linear olefins like 1-octene in alkylation reactions intracrystalline diffusion constraints can to a significant extent raise the residence time of intermediates, further enhancing the reaction in the secondary process that produces heavy polyaromatic products [11]. These cokes gradually close pore entrances and Brønsted acid sites, and activity and selectivity are lost [12, 13].

Two major post-synthesis modification strategies have been extensively investigated in order to reduce deactivation of coke and retain catalytic activity. Dealumination, which is performed by controlled acid treatment, can selectively remove the atoms of framework aluminum, and thus, can reduce the density of Brønsted acid sites (Si–OH–Al) [14]. Although this strategy is effective at inhibiting overly active secondary reactions by reducing acidity, it can also cause reduced activity of the alkylation process and degradation of the framework in stages on overly aggressive conditions [15]. Conversely, silicon atoms can be selectively removed by alkaline treatment of the structure to produce a hierarchical pore structure with mesopores and intrinsic micropores [11]. This design promotes a fast diffusion of large reactants and intermediates at the expense of leaving the original acidic functionality intact to large extent [16, 17].

Despite the large number of studies which have separately discussed the effects of dealumination or desilication on zeolite performance, there are few direct and systematic comparisons of the two types of modifications, especially in the context of coke formation during liquid-phase toluene alkylation by bulky olefins. Comparative studies that have been carried out so far have mainly concentrated on gas-phase reactions or lighter olefins in which diffusion limitations are not so intense [8]. Furthermore, the research conducted with the utilization of HY zeolites produced fully in-house with the usage of raw materials is limited, although they are crucial to achieving reproducibility and facilitating mechanistic understanding [18]. This paper aims to address some of the gaps in the

literature, synthesize HY zeolite using its constituents, perform a controlled dealumination and desilication process, and correlate the structural, textural, and acidic changes that occur with catalytic activity and coke deposition within systematic advancements. Thermogravimetric analysis (TGA) and CHNS elemental analysis were used to compare the quantities of coke deposition on spent catalysts and hence clarify the existence of direct correlations between structure and performance and deactivation in the liquid-phase alkylation of toluene with 1-octene.

## *2. Experimental*

### *2.1 Research Strategy and Engineering Framework of the Study*

It is essential to provide a brief overview of the research strategy for catalyst deactivation in aromatic alkylation reactions from a chemical engineering perspective, with a particular focus on coke formation over freshly prepared HY zeolite catalyst, as well as both acid and base-modified (i.e., dealuminated and desilicated HY zeolites catalysts). This approach relies on establishing a clear relationship between the zeolite pore structure, the distribution of acid sites, and mass transfer constraints to control coke accumulation and catalyst stability. Strongly acidic Brønsted sites promote alkylation reactions but can also accelerate secondary reactions leading to the formation of heavy hydrocarbon species.

When using bulky alkylation molecules, such as linear olefins, the restriction of diffusion within the narrow micropores increases the residence time of the reactive intermediates, thus increasing the likelihood of pre-have carbon formation (i.e., coke precursor development). In this study, coke deposition is treated as a consequence of coupled reaction–diffusion limitations and acidity effects, rather than as an isolated chemical phenomenon. Scientifically, the alkylation system involves reactions between aromatic compounds and very bulky linear olefins, imposing stringent transport requirements on the catalyst that must be met within its structure. This makes it a suitable system for testing the effects of structural framework and acidic modifications on coke formation under true limited diffusion conditions.

The overall engineering workflow of this study is represented in the diagram shown in Figure 1, which includes a brief sequence of zeolite synthesis, ion exchange, post-synthesis modification, alkylation reaction, and coke analysis. The engineering logic flows smoothly from catalyst development to performance testing, clearly aiding in the interpretation of the experimental results.

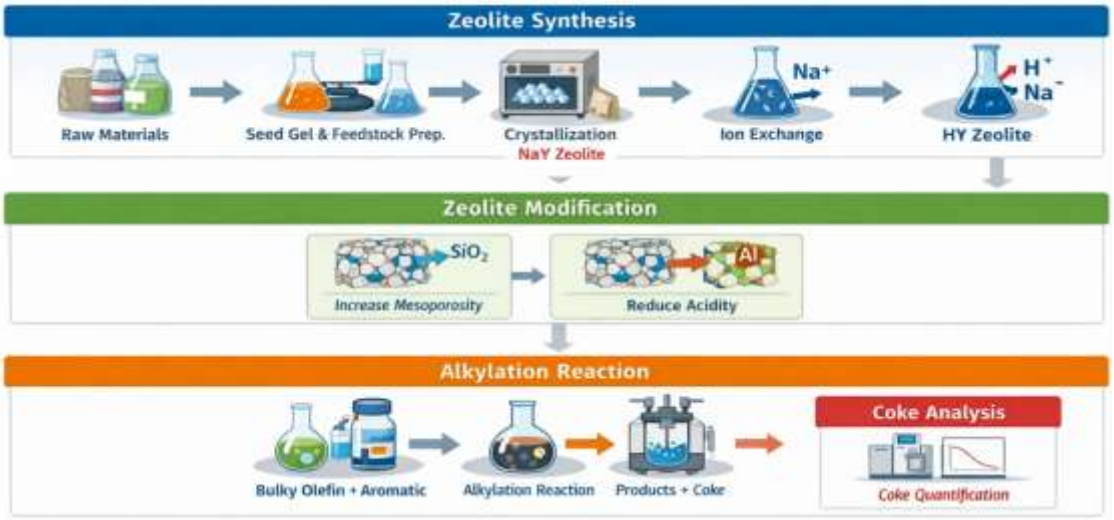
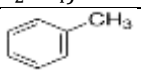


***Figure 1. Summary of the experimental laboratory workflow illustrating the synthesis and modification of a zeolite catalyst, the alkylation reaction, and the analysis of accumulated coke.***

### *2.2 Chemical Materials*

This subsection includes a description of the materials and chemical reagents used in the synthesis, ion-exchange, and post-syntheses dealuminated and desilicated modification along with subsequent testing of the catalytic properties of type Y zeolite in alkylation reactions. All chemicals were used as is, without any further purification, unless otherwise stated. Distilled water was used in all preparation, dissolution, washing, and dilution processes to minimize any impurities that might affect the crystallization, structural framework composition, or catalytic behavior of the zeolite, as recommended in published literature [19]. Table 3.1 provides a comprehensive list of all chemicals, their composition, origin, and their specific functions in the experimental work.

***Table 1. Materials and Reagents in the experimental work.***

| Material / Formula | Purity / Manufacturer | Function |
|---|---|---|
| Anhydrous Sodium aluminate: (50.9 wt.% $Al_2O_3$ + 31.2 wt.% $Na_2O$ + 17.9 wt.% $H_2O$) | ≥ 98%, analytical grade (Sigma Aldrich) | Aluminum source for Na-Y zeolite synthesis |
| Sodium hydroxide: (NaOH) | ≥ 98%, pellets (Merck) | Hydrogel preparation (Mineralizer source) and desilication agent |
| Ludox AS-40 colloidal silica | 40 wt.% $SiO_2$ suspension in water (Sigma Aldrich) | Silica source for Na-Y zeolite synthesis |
| Distilled water: ($H_2O$) | University of Technology, College of Chemical Engineering | Solvent source for zeolite synthesis and washing |
| Ammonium chloride: ($NH_4Cl$) | ≥ 99.5% (Sigma Aldrich) | Ion exchange to produce HY zeolite type |
| Sulfuric acid: ($H_2SO_4$) | 99.999% (Merck) | Dealumination treatment |
| Toluene: ($C_6H_5CH_3$)  | ≥ 99.5% (Sigma-Aldrich) | Aromatic reactant (substrate) |
| 1-Octene: $CH_2CHC_6H_{13}$ | ≥ 98% (Acros Organics) | Alkylating agent |
| n-Hexane: $CH_3(CH_2)_4CH_3$ | ≥ 99% (Merck) | Diluent for GC sample preparation |
| n-Pentane: $CH_3(CH_2)_3CH_3$ | ≥ 99% (Scharlau) | Washing of spent catalysts before TGA analysis |

### *2.3 Zeolite Y Catalyst Manufacturing and Treating Procedures*

#### *2.3.1 Zeolite Synthesis*

Sodium aluminate ($NaAlO_2$), sodium hydroxide (NaOH), colloidal silica (Ludox), and distilled water were used as the main raw materials in the preparation of Na-Y-type zeolite. Sodium aluminate served as the aluminum source necessary for the formation of the aluminosilicate framework structure, while colloidal silica (Ludox) provided a homogeneous and stable source of silicon.

Sodium hydroxide provided the alkaline medium necessary for dissolving the aluminosilicate and forming the gel that led to crystallization; it also acted as a charge-balancing cation during structure formation by supplying sodium ions. Distilled water served as the solvent and played a vital role in controlling the viscosity as well as the crystallization behavior.

These materials were used to produce both the seed gel and the feed stock gel, which together controlled the crystallization density, crystal growth rate, and phase purity of the resulting Na-Y type zeolite. Obtaining a FAU-type zeolite structure and avoiding unwanted crystalline phases required precise control of the synthesis process composition and mixing conditions, as described in the published literature [18]. Figure 2 shows a simplified diagram of the preparation procedure for Na-Y zeolite sample from its raw materials.

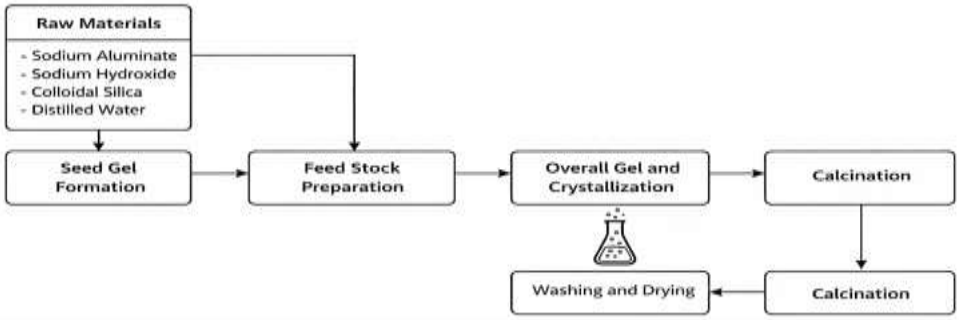



***Figure 1. Block Diagram illustrating the integrated preparation of Na-Y Zeolite from raw materials***

A typical mass of 0.9718 g of Na-Y zeolite catalyst was synthesized using the conventional hydrothermal method from its raw materials [20, 21]. The manufacturing steps included seed gel and feed stock preparations, and then overall gel formation, followed by crystallization, washing, and drying, as described in chemical recipe for FAU-structure found in the verified syntheses of zeolite materials handbook. The molar formulas of the material required for the zeolite synthesis are given as follows: Type Material: $Na_{56}$ [$Al_{56}$ $Si_{136}$ $O_{384}$]: 250 $H_2O$.

$$\boldsymbol{Feed\ stock\ gel}: (\mathbf{95\%}\ \boldsymbol{Al}): \mathbf{4.30}\boldsymbol{Na_2O}: \boldsymbol{Al_2O_3}: \mathbf{10}\boldsymbol{SiO_2}: \mathbf{180}\boldsymbol{H_2O}$$

$$\boldsymbol{Seed\ gel}: (\mathbf{5\%}\ \boldsymbol{Al}): \mathbf{10.67}\boldsymbol{Na_2O}: \boldsymbol{Al_2O_3}: \mathbf{10}\boldsymbol{SiO_2}: \mathbf{180}\boldsymbol{H_2O}$$

$$\boldsymbol{Overall\ gel}: \mathbf{4.62}\boldsymbol{Na_2O}: \boldsymbol{Al_2O_3}: \mathbf{10}\boldsymbol{SiO_2}: \mathbf{180}\boldsymbol{H_2O}$$

Initially, an appropriate amount of sodium aluminate ($NaAlO_2$) and sodium hydroxide (NaOH) were completely dissolved in distilled water with continuous stirring. Colloidal silica (Ludox, $SiO_2$) was then slowly added to the solution inside a plastic bottle, and the mixture was magnetically stirred for approximately 10 minutes to obtain a homogeneous aluminosilicate gel. The seed gel prepared in this way was left to age at room temperature for 24 hours, which helped stabilize the nuclei [22]. Alternatively, sodium aluminate and sodium hydroxide were also dissolved inside deionized water in another plastic bottle, and colloidal silica was then added to prepare the feed stock gel. The mixture was stirred for approximately ten minutes until a smooth gel was formed [19]. A measured amount of seeding gel was slowly added to the feed stock gel with continuous stirring to form the micro-synthetic gel, which was then continuously stirred for 20 minutes to achieve complete homogeneity. Secondly, this overall microgel was then placed in plastic bottle where it underwent hydrothermal crystallization at 100 °C for a specified time of 18 hours [23]. The samples were taken out of the oven and centrifuged for 10 minutes. The resulting solid products were washed several times with distilled water until the pH of the suspensions reached approximately 8, indicating the removal of excess alkalinity. The

washed samples were then oven-dried at 100 °C overnight to obtain Na-Y zeolite powder. The synthesized Na-Y zeolite was subsequently applied in ion-exchange and then post-synthetic modification steps to get the protonated and modified forms of Y-catalyst used in subsequent alkylation reaction. Furthermore, the reaction which aluminosilicate precursor species produced within the alkaline medium can be represented by the following simplified reactions [24]:

1- Dissolution of alumina species in alkaline medium:

$$\mathbf{NaAlO_2 + H_2O \rightarrow Al(OH)_4^- + Na^+} \quad \mathbf{(1)}$$

2- Silica hydrolysis and interaction with aluminate species:

$$\boldsymbol{SiO_2 + 2OH^- \rightarrow SiO_3^{2-} + H_2O} \quad \mathbf{(2)}$$

3- Formation of alumina-silicate precursor species:

$$\mathbf{Al(OH)_4^- + SiO_3^{2-} \rightarrow Al\text{-}O\text{-}Si\ (gel\ network)} \quad \mathbf{(3)}$$

It should be noted that aluminosilicates remain in a reactive and soluble form within the alkaline feed stock medium to allow reaction with seed nuclei. The main chemical reaction represented the stabilization of aluminate species in alkaline solution can be shown as follows [25]:

$$\mathbf{Al(OH)_4^- \rightleftharpoons Al(OH)_4^-\ (soluble\ species)} \quad \mathbf{(4)}$$

The reaction representing the chemical composition required for the growth of the aluminosilicate framework on the seed nuclei during the hydrothermal crystallization of FAU-type zeolite can be formulated as follows [26]:

$$\mathbf{Seed\ nucleus + Al\text{-}O\text{-}Si\ gel\ species \xrightarrow{\Delta} growth\ of\ FAU\ structure} \quad \mathbf{(5)}$$

### *2.3.2 Ion Exchange Treatment*

Synthesized Na-Y zeolite contains sodium ions to neutralize the negative charge of the aluminum within its framework structure. These sodium ions must be replaced by protons to form Brønsted acidic sites [27]. In this study, ammonium chloride (i.e., an aqueous solution of $NH_4Cl$ salt) was used in an ion-exchange process. A concentration of 0.5 M, which would ensure sufficient ammonium ions ($NH_4^+$) for complete exchange with sodium ions ($Na^+$) present within the zeolite framework, was chosen to convert the synthesized Na-Y zeolite form to $NH_4$Yform, followed by thermal activation to obtain the protonated HY form [28]. Upon subsequent thermal treatment, the ammonium species decompose to provide well-distributed protonated sites within the zeolite structure. The ion exchange process was repeated many times to ensure the efficient replacement of sodium ions with ammonium ions. This provides controlled activation of the acidity while preserving the FAU crystal structure of the Y-type zeolite. The overall transformation from Na-Y to HY can be represented as follows [29]:

$$\mathbf{Na\text{–}Y \xrightarrow{NH_4^+\ exchange} NH_4\text{–}Y \xrightarrow{thermal\ activation} H\text{–}Y} \quad \mathbf{(6)}$$

Practically, ammonium chloride was weighed using an analytical balance and then dissolved in distilled water. The solution was stirred using a magnetic stirrer to ensure complete dissolution of the salt and to obtain a clear, homogeneous solution. Distilled water was used to avoid introducing extraneous ions that could interfere with the ion exchange process. The prepared ammonium chloride solution was allowed to reach a temperature of 80 °C, and then the laboratory-prepared Na-Y zeolite was added to form a solid-liquid suspension (i.e., about 1 g of zeolite placed in 100 mL ammonium chloride solution). Stirring continued (6 rpm) at this temperature for approximately one hour to ensure effective contact between the zeolite particles and the ammonium ions within the aqueous solution.

At the end of the first ion exchange cycle, the solid $NH_4$Y zeolite was separated from the solution by centrifugation and thoroughly washed with distilled water to remove any remaining sodium and chloride ions. The extracted solid then directly underwent a second

ion exchange cycle under similar conditions. It is worth noting that this two-step ion exchange process increases the degree of sodium removal and results in a more homogeneous distribution of ammonium ions within the zeolite structure. Finally, the ammonium-exchanged zeolite was collected from the liquid phase by centrifugation after the final cycle and then dried in a laboratory oven at 110 °C for an extended period to remove physically adsorbed water and any residual moisture. Drying at a moderate temperature helps stabilize the ammonium-exchanged structure before thermal activation and prevents any uncontrolled structural transformation during calcination. The ion-exchange process occurring during this step can be represented as follows [30]:

$$\mathbf{Na\text{-}Y} + \mathbf{NH_4^+} \rightleftharpoons \mathbf{NH_4\text{-}Y} + \mathbf{Na^+} \quad \textbf{(7)}$$

The calcination process was then carried out at 300-400 °C as the final stage to obtain the protonated form. During this stage, ammonia gas was removed by the thermal decomposition of ammonium ions (i.e., ammonia $NH_3$ is probably liberated outside the zeolite framework) to generate the catalytically active HY form of zeolite catalyst, which is necessary for the alkylation reactions. The conversion of the ammonium-exchanged zeolite to its protonated form during calcination can be represented as follows [31]:

$$\mathbf{NH_4\text{-}Y} \xrightarrow{\Delta} \mathbf{H\text{-}Y} + \mathbf{NH_3} \uparrow \quad \textbf{(8)}$$

### *2.3.4 Post-Synthesis Modification of HY Zeolite*

As previously mentioned, HY zeolite underwent two different post-synthetic chemical treatments to control its acidity and pore structure. The first treatment involved dealumination, using specific temperature and contact time conditions to partially remove aluminum from the structure, thus reducing the excess density of acidic sites [32]. The second treatment was desilication, where silicon atoms were selectively removed from the structure, modifying the pore structure and increasing diffusion accessibility [33]. In fact, the protonated form of HY zeolite after ion exchange and calcination has a high density of acidic Brønsted sites, making it very suitable for alkylation reactions, but simultaneously increasing catalyst deactivation due to coke formation. HY zeolite with high aluminum content is associated with a high concentration of acid sites, typically more than 0.8–1.0 mmol $H^+ \cdot g_{cat.}^{-1}$, which can accelerate oligomerization and condensation reactions leading to coke deposition [34]. On the other hand, because of the large size of the olefin molecules, the micropore structure, with a pore diameter of approximately 0.74 Å, limits diffusion [35]. Therefore, post-synthesis modifications were applied as an engineering approach to control the acidity of the material and the accessibility of its pores (i.e., mesoporation through the microporosity of the catalyst structure), while preserving the FAU structure.

### *2.3.5 Dealumination of HY Zeolite*

Dealumination treatment has been used as a post-synthesis modification strategy while preserving structural integrity. The chemical process of dealumination during acid leaching can be simplified as follows [14]:

$$\mathbf{Al\text{–}O\text{–}Si} + \mathbf{H^+} \rightarrow \mathbf{Al_{(aq)}^{3+}} + \mathbf{Si\text{–}OH} \quad \textbf{(9)}$$

This involves breaking the Al–O bonds within the zeolite structure and forming silanol groups at defect sites, resulting in reduced acidity and modified pore characteristics. In fact, the proton diffusion into the channels of zeolite and interaction with Al–O–Si linkages result in partial removal of framework aluminum [15, 36]. A dilute sulfuric acid solution was prepared by adding 5 g of $H_2SO_4$ to 100 mL of distilled water. One gram of HY zeolite was then added to the dilute acid solution to form a solid-liquid suspension. The sample was then placed on a magnetic stirrer and left at 50 °C with continuous stirring for 30 minutes. These conditions were chosen to allow for the partial selective extraction of aluminum atoms from the catalyst structure without causing excessive framework collapse. The continuous stirring helps in maintaining the uniform exposure of zeolite

particles to the acidic medium so that there is minimum gradient of concentration within the suspension. The dealuminated HY (De-Al-HY) zeolite was separated from the acid solution after the treatment was completed by centrifugation. The recovered material was washed several times with distilled water to remove any residual acid and the aluminum species dissolved during the dealumination process until the washings reached near-neutral pH values, indicating effective removal of acid residues. The acid-modified zeolite was then dried overnight at 110 °C. This material was stored under dry conditions prior to structural characterization and catalytic testing.

### *2.3.6 Desilication of HY Zeolite*

The desilication of HY zeolite was performed to selectively remove structural silicon and introduce additional intermediate porosity (i.e., mesoporosity) within the zeolite crystals [37]. This modification was implemented to enhance pore accessibility and mass transfer, particularly in alkylation reactions involving macro or bulky-olefin molecules, while preserving the overall structure of FAU. The chemical process associated with desilication during alkali treatment (i.e., base leaching) can be simplified as follows [38]:

$$\mathbf{Si{-}O{-}Si + 2OH^- \rightarrow SiO_3^{2-} + Si{-}OH} \qquad \mathbf{(10)}$$

This reaction is assumed to break the Si–O bonds within the zeolite lattice, with the accompanying formation of defect sites that ultimately lead to increased mesoporosity and improved diffusion properties [39]. In more detail, hydroxide ions selectively attack Si–O–Si bonds within the zeolite structure, a process of partial dissolution of silicon species that simultaneously forms secondary mesopores. Uniform exposure of all zeolite particles to the alkaline medium, ensured via stirring, minimizes the probability of over-desilication at specific locations within the sample. The desilication process was carried out in a dilute alkaline solution. A sodium hydroxide solution was prepared by dissolving 0.5 g of sodium hydroxide in 250 mL of distilled water. 1.0 g of HY zeolite was added to 100 mL of the prepared alkaline solution to form a solid-liquid suspension, which was then placed on a magnetic hotplate stirrer and treated at 50 °C with continuous stirring for 30 minutes [40]. These conditions were specified for controlled silicon extraction with minimal damage to the Y-lattice. The desilicated HY (De-Si-HY) zeolite was separated from the liquid phase (i.e., alkaline solution) after the treatment was complete by centrifugation. The material recovered was washed several times with distilled water to remove residual alkali and soluble silicate species, until the pH of the supernatant became almost neutral. It was then dried overnight in a laboratory oven at 110 °C to remove residual moisture and stabilize the modified

## *2.5 Testing the Performance of Catalysts in Alkylation Reactions*

### *2.5.1 Reaction Conditions, Catalysts, and Reactants Used in Alkylation*

After the ion exchange, dealumination and desilication processes were completed, the modified zeolite samples were prepared for use in alkylation reaction experiments. The HY, De-Al-HY, and De-Si-HY zeolite catalysts were all subjected to a final drying step at 100-110 °C to remove physically adsorbed water before being studied in reaction experiments. The exact weight of each catalyst was recorded prior to its direct introduction into the reaction system. The aromatic and alkylating reactants were respectively toluene ($C_6H_5CH_3$) as the aromatic substrate and 1-octene ($C_8H_{16}$) as the alkylating agent. The two reactants were chosen to represent an alkylation system with a bulky linear olefin molecule, which would be assumed to have diffusion limitations inside the microporous structure of zeolites [2].

Different molar ratios in the feed between toluene and 1-octene of 4:1, 7:1, and 10:1 were experimented on so as to study their effect on catalytic operation together with coke formation behavior. The volumes of the reactants were determined based on the density

and the number of moles. For example, to achieve a 4:1 molar ratio, a 1000 µL micropipette was used, yielding a total toluene volume of 7330 µL by adding 330 µL to seven full strokes of the syringe. The total volume of 1-octane was 1832 µL, with 832 µL added for one full stroke. The toluene and octane-1 were weighed separately and then mixed in the reaction flask.

The reaction temperature varied within the range of 90-110 °C. Operating at a temperature within this range ensures that the alkylating agent remains in a liquid state, thus preventing excessive evaporation and stabilizing the reaction conditions [5]. On the other hand, catalyst masses of 0.15, 0.25, and 0.35 g were used. These values were chosen based on a constant reaction volume of 10 mL.

Based on prior experimental testing, using less than these amounts resulted in insufficient catalytic activity, while using larger amounts of catalyst caused mixing difficulties and reduced mass transfer efficiency within the batch reactor. Therefore, the selected catalyst masses represent a suitable balance between catalytic performance and efficient mixing. Figure 3 presents a schematic block diagram summarizing the catalyst preparation and reaction process to illustrate the overall experimental sequence in this study.

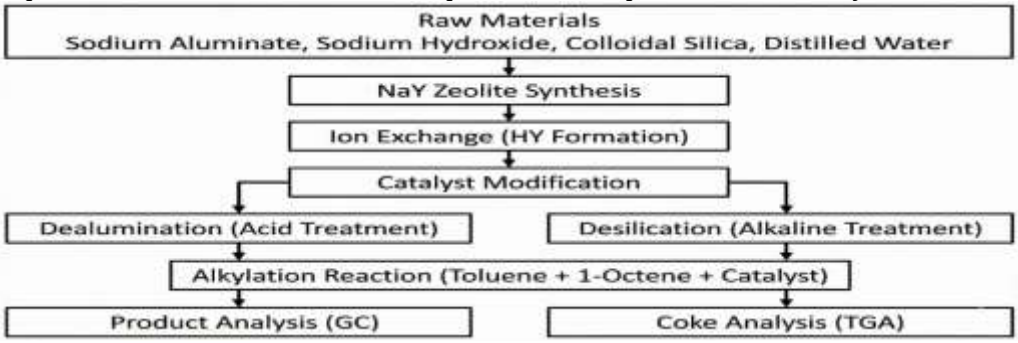



**Figure 3. Comprehensive flowchart demonstrating the preparation of catalysts and alkylation reactions.**

### 2.5.2 Experimental Setup, Reactor Configuration, and Alkylation Reaction Scheme

The alkylation reaction was carried out in a batch reactor system using laboratory-prepared and activated zeolite catalysts. A small, round-bottomed reaction flask was placed inside a larger flask containing paraffin oil, which served as an oil bath to ensure uniform and stable temperature control. The larger outer flask also helped to minimize heat loss from the system to the surrounding atmosphere, as the reaction is exothermic. This flask was heated using a magnetic stirrer with heating capabilities. A small magnetic rod was placed inside the reaction flask to ensure exhaustive mixing of the reactants and catalyst. The reaction flask was also equipped with a reflux condenser (i.e., reflux conditions) to prevent the loss of volatile reactants during operation. Figure 3 elucidates a schematic flow diagram of alkylation experimental rig. Additionally, to provide a detailed overview of the steps in the alkylation reactions, a simplified representation of the process can be presented as follows:

Input: “toluene,1-octene and Y catalyst". It should be noted that 1-octene was chosen as an alkylating agent for toluene alkalinity due to its reasonable price and commercial availability. Furthermore, it acts as a bulky olefin, allowing for the study of diffusion effects and, simultaneously, the determinants of coke formation behavior within Y-type zeolite catalysts). Output: including the following products: desired product: “2-octyltoluene” and undesired product: “3-octyltoluene, 4-octyltoluene"; "2-octene, 3-octene, 4-octene"; and "heavy residue”.

The reaction begins by heating up the entire system to the reaction temperature (i.e., 90 or 100, or 110°C). Once the desired temperature is reached, the reaction is left to proceed

under continuous stirring. At the end of the reaction time, heating is stopped, and the reaction flask is carefully disconnected from the condenser. The reaction is also immediately quenched by placing the reaction flask in an ice bath for ten minutes to cool it rapidly and prevent any side reactions that might be occurring within it. After cooling, the reaction mixture was poured into another clean container and left to separate into two phases (i.e., the solid catalyst and the liquid reactants). The liquid phase was separated, and approximately 1 mL of the liquid reaction products were taken using a micropipette, mixed with 0.1 mL of normal hexane to reduce sample viscosity, sealed tightly, and finally stored at -4 °C in order to minimize evaporation losses as well as any chemical degradation or change in composition prior to analysis. This dilution would minimize possible injector fouling and improve peak shape during later GC measurement. Meanwhile, the remaining solid phase was washed with normal pentane in a glass beaker with stirring, without heating, for approximately 15 minutes to remove physically adsorbed hydrocarbons. This makes sure that in the later TGA analysis, any weight loss can be solely attributed to carbonaceous deposits formed during catalysis and not due to volatile or weakly bound species [11]. The spent catalyst was then filtered through filter paper, dried, and collected as a solid powder for later use in determining the amount of accumulated coke using TGA analysis. The same reaction procedures described above were applied to all three different molar ratios, temperatures, and catalyst masses. Therefore, a total of nine experiments were conducted for each type of Y-catalyst. The optimal reaction conditions were determined based on conversion performance, selectivity, and coke buildup.

The conversion of 1-octene (%) was calculated using the following expression:

$$\mathbf{Conversion_{octene}} = \frac{F_{\text{octene,in}} - F_{\text{octene,out}}}{F_{\text{octene,in}}} \times 100 \qquad (11)$$

While the selectivity to alkylated aromatic products (%) was determined as:

$$\mathbf{Selectivity_{alkylated}} = \frac{\sum F_{\text{alkylated products}}}{\sum F_{\text{all products}}} \times 100 \qquad (12)$$

Where F represents the molar fraction of each component determined from GC peak areas after response factor correction.

On the other hand, the total coke content was calculated from the mass loss in combustion of carbonaceous deposits while heating in an oxidizing atmosphere [38]:

$$\mathbf{Coke\ (wt.\%)} = \frac{m_{\text{before}} - m_{\text{after}}}{m_{\text{before}}} \times 100 \qquad (13)$$

Where $m_{\text{before}}$represents the mass of the dried spent catalyst prior to combustion, and $m_{\text{after}}$corresponds to the remaining inorganic mass after complete oxidation at 800°C (i.e., removal of carbonaceous species).

### *2.6 Catalyst Characterization*

The complementary techniques were used to analyze the structural and textural properties. The crystallinity and framework integrity were evaluated by recording the X-ray diffraction (XRD) patterns on a STOE STADI P diffractometer using Cu K 1 radiation. FTIR was used to determine the framework vibrations and hydroxyl groups by using a Gasco 4200 spectrometer. SEM-EDX (Quanta 200) at 15 kV and x 500 were used to study morphology and elemental surface composition. The XRF was used to measure bulk Si/Al ratios using a PANalytical Zetium spectrometer. Measurements of Nitrogen adsorption desorption isotherms were performed at 77K in a Quantachrome Nova 2200E system. The BET method was used to calculate specific surface area and adsorption data were used to compute pore volume and micropores.

### *2.7 Alkylation Reaction*

A batch reactor was used in this study to perform liquid-phase toluene alkylation with 1-octene in a round-bottom flask, immersed in a thermostatically controlled paraffin oil bath, fitted with a reflux condenser and magnetic stirring (see Figure 4). The parameters

of the reaction were systematically varied: toluene:1-octene molar ratios (4:1, 7:1, 10:1), temperatures (90, 100, 110 ◦ C), catalyst mass (150-350 mg), and reaction duration (0-300 min). Following every run, the reaction mixture was cooled in an ice bath and diluted with n-hexane and stored at -4 C before analysis. The GC-FID was used to quantify the composition of the product and 1-octene conversion utilizing Restek Rxi-5HT capillary column, where quantitative analysis was performed using corrected response factors.

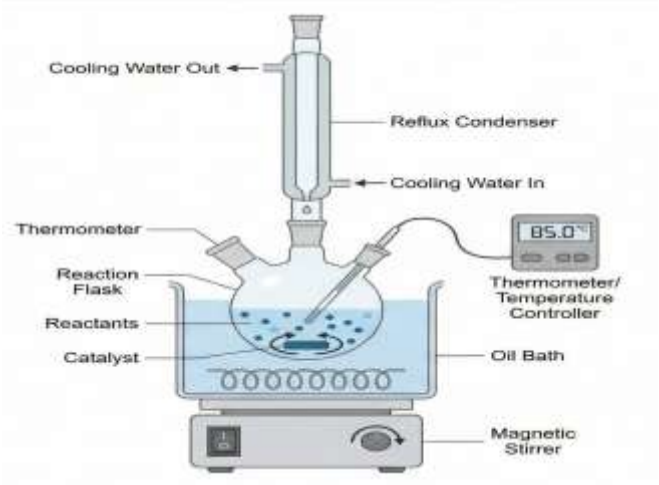



***Figure 4. A diagram illustrating a batch alkylation system.***

### *2.8 Coke Analysis*

The spent catalysts were washed using n-pentane to eliminate physisorbed hydrocarbons, filtered and dried before analysis. TGA was carried out using a Q600 analyzer in the presence of dry air (30 mL/min -1) at a heating rate of 1.25 °C/min -1 up to 800 °C. The soft coke was considered to cause weight loss between 200-400 °C whereas the hard coke was considered as causing weight loss between 400-800 °C. The analysis of carbon and hydrogen content, as well as the determination of the H/C ratio of a coke deposit, were performed by Complementary CHNS elemental analysis (Thermo Scientific FlashSmart).

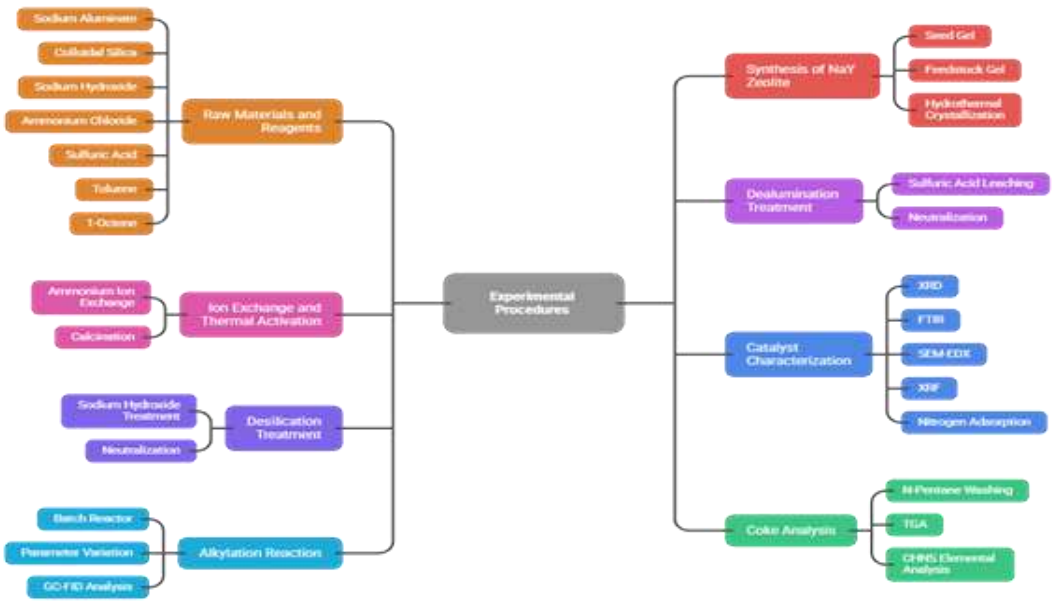


***Figure 5. Experimental workflow for the synthesis, modification, characterization, and catalytic evaluation of HY zeolite in toluene alkylation.***

## *3. Results and Discussion*

### *3.1 Comprehensive Catalyst Characterization and Structural Analysis*

Characterization studies were conducted in depth with fresh, dealuminated and desilicated HY zeolite catalysts and several other different methods of analysis which are complimentary to each other. These are X-ray diffraction (XRD) to understand crystalline phase, structural perfection, Fourier transform infrared spectroscopy (FTIR) to understand framework vibration and hydroxyl group, scanning electron microscopy (SEM) to understand morphology and hierarchical pore structure. X-ray fluorescence (XRF) and energy-dispersive X-ray spectroscopy (EDX) to understand element composition and Si/Al ratio, nitrogen adsorption-desorption analysis (BET-surface area) to understand comprehensive pore characterization. In addition to thermogravimetric analysis to verify the quantity and type of coke deposited on the catalysts as a result of alkylation reactions occurring on their surface. The multi-technique method provides complementary information, which allows a thorough assessment of the structure, composition, acidity, and porosity of the catalyst.

#### *3.1.1 X-ray Diffraction: Crystalline Structure and Framework Integrity*

X-ray diffraction (XRD) is a methodology that could provide data on the structure of crystals and also the arrangement of longer-range atoms. Figure 6 shows XRD patterns of all three of the catalysts. The peak intensities in desilicated HY are considerably larger than in fresh and dealuminated ones, which reveals that it possesses a much better crystallinity and long-range structural ordering. The unusually high crystallinity indicates the existence of minimal lattice defects and brilliant three-dimensional structural order that are traits highly sought after in applications that are related to catalysis [41]. Fresh HY exhibits moderate crystallinity that is the trait of unmodified Y-zeolite. Conversely, HY dealuminated displays widening of peaks and reduced intensities, which agrees with the literature assertions that dealumination of acids introduces flaws in the framework and reduced structural order [42]. The findings of the XRD experiment give it a rich abundance that desilication preserves or enhances the stability of the crystalline structure and dealumination impairs it**.**

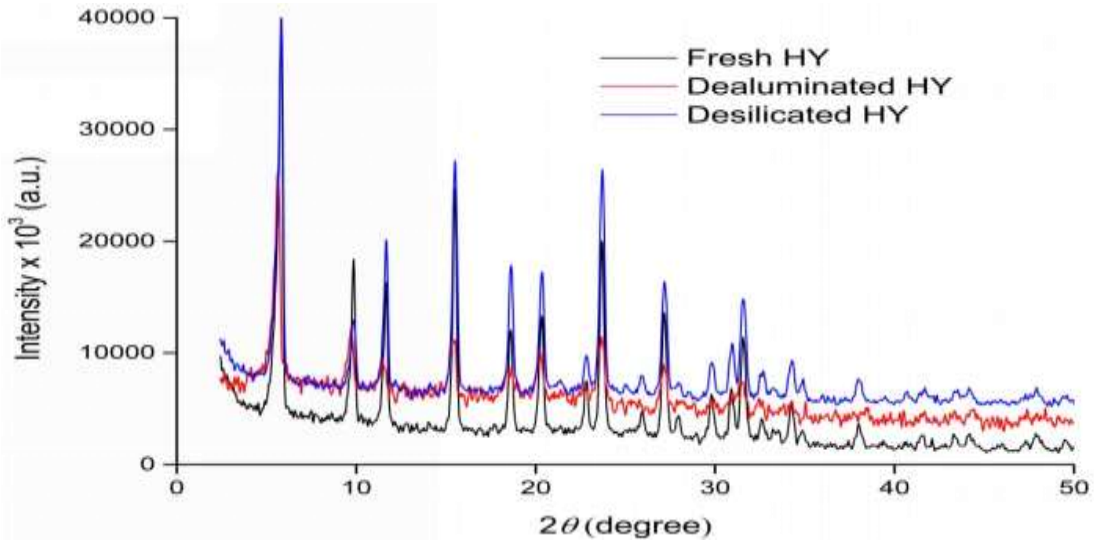


***Figure 6. X-ray diffraction patterns of fresh, dealuminated, and desilicated HY zeolites.***

### *3.1.2 FTIR Spectroscopy: Framework Composition and Hydroxyl Groups*

Fourier transform infrared spectroscopy (FTIR) reveals the structures of both the frameworks and functional groups. Figure 7 shows the FTIR spectra. The absorption bands in the 453-490 $cm^{-1}$ region can be traced back to the T-O bending mode (i.e. Si-O/Al-O). The observed band in the 715-816 $cm^{-1}$ region is attributed to the T-O-T symmetric stretching. The FTIR spectra also displays the characteristic stretching vibrations of Si-O and Al-O in the range of 1000-1300 $cm^{-1}$, and the hydroxyl stretching vibrations (i.e. OH: hydrogen bonded to the oxygen ions of the lattice structure) in the range less than 3000 to more than 3500 $cm^{-1}$. The hydroxyl stretches of the structure comprise contributions of Brønsted acid sites (Si-OH-Al bridges), water, as well as silanol groups. The presence of sharp and well-defined absorption bands in the desilicated HY demonstrates high degrees of framework integrity and minimum flaws. When fresh HY is present, the absorption intensities of HY-zeolite that have not been changed are modest [43-45]. However, when HY is dealuminated, the bands become many more and less distinct, a characteristic of dysfunction in the framework. The FTIR spectroscopy method reveals the framework structures of each of the catalysts in order to preserve the zeolite lattice, which serves as the core of the catalytic activity. It has been shown that moderate chemical modification is sufficient to preserve the lattice structure, and the greater the concentration of acids or bases used to improve the structure of the catalysts, the greater the chance of the structure collapse.

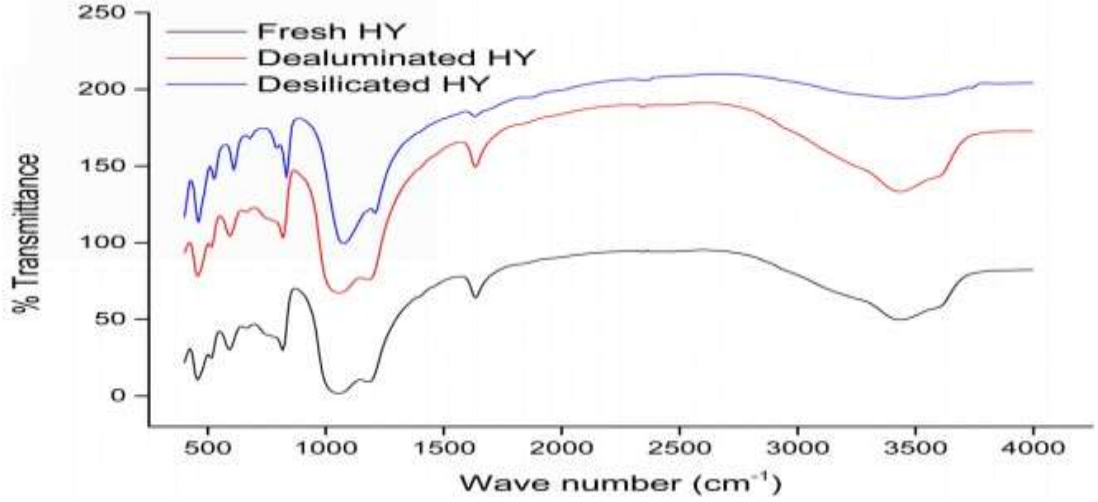
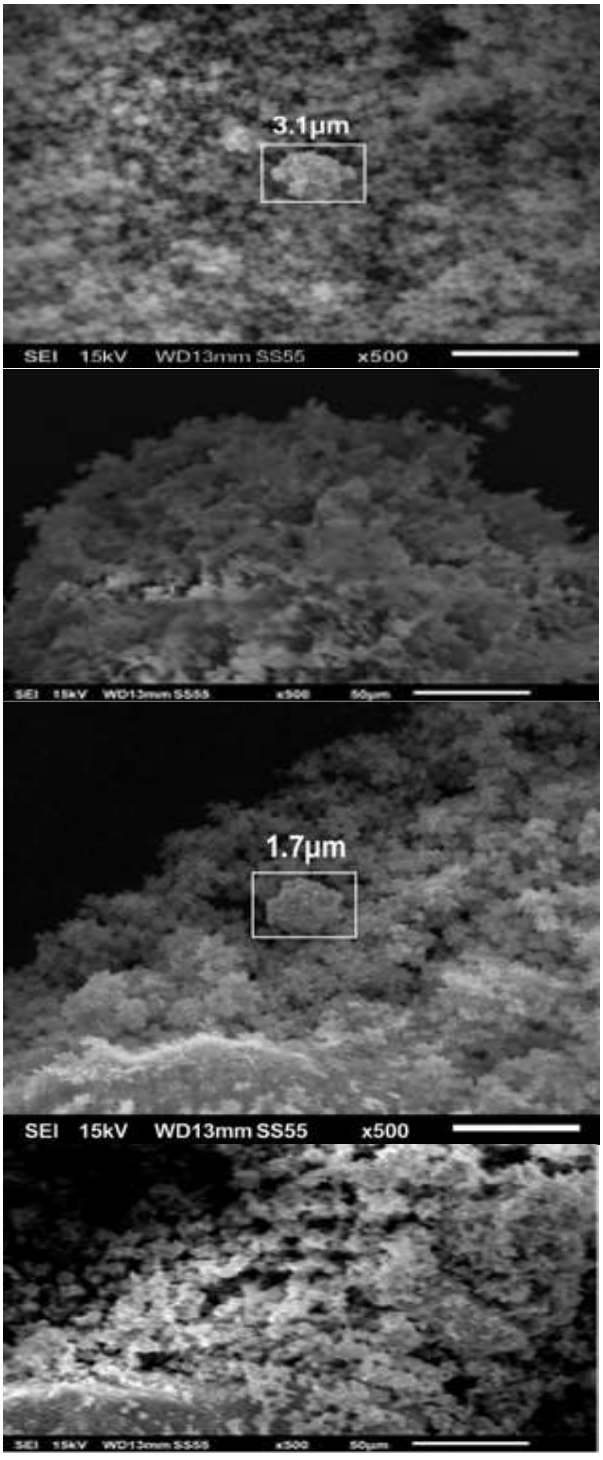



***Figure 7. Fourier transforms infrared spectra of the three HY zeolite catalysts.***

### *3.1.3 Scanning Electron Microscopy: Morphology and Hierarchical Pore Development*

Scanning electron microscopy (SEM) provides first-hand evidence of the size of particles and structural morphology. Figure 8a reveals that fresh HY has dense and smooth surfaces to particles, which are characteristic of microporous-only zeolite. Moreover, the crystal structure does not contain any visible mesopores. Figure 8b shows that dealuminated HY has rougher surfaces, that is, they have evident surface flaws and partial etching. These features indicate the change in structure through the action of acids and some porosity formation. Nevertheless, these features do not evenly distribute, and signs indicate structural degeneration [46, 47].

As shown in Figure 8c, desilicated HY has a strongly formed hierarchic network of mesopores that is defined by high interconnected cavities within the structure. Moreover, there is uniform dispersion of the desilicated HY that means that desilication process was controlled, and the structural integrity of the particles was maintained [33, 48]. The hierarchical pore structure that comprises of micropores and mesopores that are complementary to each other comes with the most desirable mass-transfer characteristics.



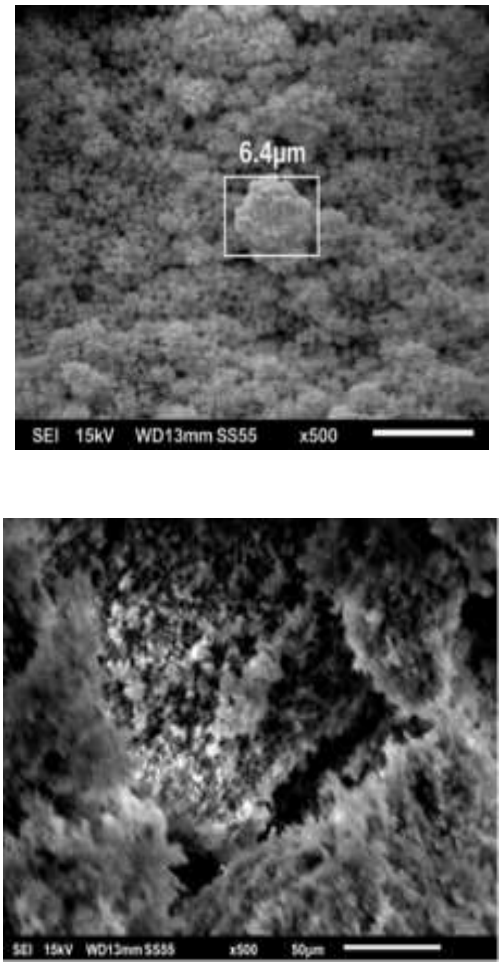



***Figure 8: SEM images of (a) Top: Fresh HY which has smooth, microporous structure, (b) Middle: Dealuminated HY which has etched surface with non-uniform porosity, and (c) Bottom: Desilicated HY which has hierarchical network of mesopores.***

Furthermore, as can be seen in Figure 8, the fresh HY zeolite particle aggregates consist of semi-cubic and spherical crystals with lengths up to 3.1 µm, which are non-agglomerated. Despite chemical treatment, the zeolite crystals appear more distinct and homogeneous. Acidic treatment resulted in a shrinkage of the dealuminated HY zeolite structure, with average particle diameters reaching 1.7 µm, while alkaline treatment led to an expansion of the desilicated HY zeolite structure, with average particle diameters reaching 6.4 µm.

### *3.1.4 Elemental Composition and Si/Al Ratio*

X-ray fluorescence (XRF) and energy-dispersive X-ray spectroscopy (EDX) are used to determine the percentage of elements within samples. The values of the bulk Si/Al ratio of dealuminated HY are 5.3 and 4.9 using XRF and EDX respectively, meaning that a significant amount of aluminum has been removed. The rise in the Si/Al ratio is in agreement with those values reported in the scientific literature of acid-dealuminated Y-zeolites [14], which stand between 5.0 and to more than 5.5 (inclusive).

The loss of aluminum leads to an immediate decrease in the concentration of Brønsted acid sites which eventually leads to a decrease in the efficiency of the catalytic process. With desilicated HY, the silicon/aluminum ratios read 4.0 (XRF) and 3.7 (EDX), meaning that there has been selective silicon removal and relative enrichment of the aluminum,

respectively. Published data on hierarchical zeolites indicate that the Si/Al ratio ranges between 3.8 and 4.2 [49], and the data obtained from this study are in good agreement with those data in the literature. The importance of a lower ratio of silicon to aluminum in the semiconductor material, such as zeolite, is a higher acid site density per unit mass. A decrease in this ratio indicates a higher aluminum content and an increase in the number of Brønsted acid sites, as the silicon-to-aluminum ratio directly affects the concentration of these sites. Silicon to aluminum ratios in parent HY remain unchanged during the process at 4.5 (XRF) and 4.0 (EDX). The good agreement between XRF and EDX confirms the regularity of the composition and reliability of the measurements, and the variances of the measurement are less than half the total.

***Table 2. Si/Al ratios and acidity levels of zeolite catalysts.***

| Sample | Si/Al (XRF) | Si/Al (EDX) | Acidity |
|---|---|---|---|
| Fresh HY | 4.5 | 4.0 | Moderate |
| Dealuminated HY | 5.3 | 4.9 | Low |
| Desilicated HY | 4.0 | 3.7 | High |

### *3.1.5 Textural Properties: Surface Area, Pore Volume, and Mass Transfer*

The Brunauer-Emmett-Tiller (BET) method, based on the physical adsorption of nitrogen gas at 77 K, enables the discovery of key information relating to pore volume and surface area of catalysts. The shape of the adsorption or desorption branch may be mechanistically attributed to the pore structure of a solid. Such that the analysis of the adsorption-desorption hysteresis loop is essential in order to get a complete picture about the main structure of the pores within the sample. The formation of mesopores, less micropores, within the structure normally gives rise to adsorption-desorption hysteresis loops. Generally, a total pore volume of solid "adsorbent surface" can easily be found, if the density of gas "adsorbate" is known.

Desilicated HY has the highest surface area ($S_g$ = 700.5 $m^2/g$) and pore volume (0.344 $cm^3/g$) and is greater than fresh HY. Moreover, the obtained results agree perfectly well with the literature on the hierarchical zeolites, a range of 690-750 $m^2/g$ and 0.33-0.36 $cm^3/g$ [50]. The hierarchical growth strongly supports the fact that the mesopore volume increases to 0.042 $cm^3/g$, which is larger than the mesopore volume of fresh HY (i.e., 0.036 $cm^3/g$), This is achieved by a difference in the value of (d), which represents the spacing between parallel planes in the atomic lattice, within a range of approximately (0.25 angstroms), consistent with estimates published in the scientific literature, which range between 0.040 and 0.050 $cm^3/g$ [51]. In addition, in the stage of introducing a secondary transport network, the preservation of the micropore volume (i.e., 0.302 $cm^3/g$ = fresh HY of 0.301 $cm^3/g$) demonstrates that the main acid sites remain unchanged. On the other hand, and according to the literature, dealuminated HY has the lowest textural properties with the lowest surface area of 538.8 $m^2/g$, and the lowest pore volume of 0.309 $cm^3/g$. This aligns with the observation of significant structural integrity loss (equivalent to 15–25% of the material from which aluminum is acid-dealuminized) [52]. Compared to traditional Y-zeolite, laboratory-prepared zeolite HY has some middle, though satisfactory qualities with a particular value of 687.6 $m^2/g$ and 0.337 $cm^2/g$. In fact, hierarchical mesoporosity has important advantages to prevent the accumulation of intermediates and coke. The textural characteristics have direct control over the accessibility of reactants to acid locations and product release rates.

***Table 3: Textural characterization of zeolite catalysts.***

| Sample | $S_g$ ($m^2/g$) | $V_{total}$ ($cm^3/g$) | $V_{mic}$ ($cm^3/g$) | d (Å) |
|---|---|---|---|---|
| Fresh HY | 687.6 | 0.337 | 0.301 | 6.81 |
| Dealuminated | 538.8 | 0.309 | 0.281 | 6.83 |
| Desilicated | 700.5 | 0.344 | 0.302 | 7.05 |

### *3.1.6 Coke Formation and Catalyst Deactivation*

Thermogravimetric analysis (TGA) is a method of thermal analysis [11]. It measures weight/mass change (loss or gain) and the rate of weight change as a function of temperature, time and atmosphere. Coke is created during all transformations of the hydrocarbon compounds and is a secondary product from a sequence of reaction steps that take place in the catalytic alkylation. Coke is generally a mixture of heavy side products. Chemically, two types of coke components are deposited on the surface of the catalyst during alkylation reactions: light coke (i.e., non-polyaromatic) and heavy coke (i.e., polyaromatic). The percentage of coke was determined using equations 14 and 15:

$$\boldsymbol{coke}\%\ (\boldsymbol{soft}) = \frac{\boldsymbol{W_{200}-W_{400}}}{\boldsymbol{W_{400}}} \times \mathbf{100} \qquad \textbf{..... (14)}$$

$$\boldsymbol{coke}\%\ (\boldsymbol{hard}) = \frac{\boldsymbol{W_{400}-W_{800}}}{\boldsymbol{W_{800}}} \times \mathbf{100} \qquad \textbf{..... (15)}$$

Where $W_{200}$, $W_{400}$ and $W_{800}$ are the weights of the zeolite samples at temperatures of 200°C, 400 °C and 800 °C, respectively. Soft coke was estimated to be within the temperature range of 200–400 °C, while hard coke was estimated to be within the temperature range of 400–800 °C [53]. In all three zeolite samples, the percentage of hard coke was higher than that of soft coke. TGA analysis showed that both modified zeolite samples had a lower coke content compared to the unmodified fresh HY-zeolite sample, indicating that the dealumination treatment reduced acidity and the percentage of precipitated coke, while the desilication treatment increased the average porosity (i.e., mesoporous) and further reduced the precipitated coke. Deposits of coke causing deactivation can be measured thermogravimetrically of wasted catalysts, as shown in Table 4 (a). It was found that the amount of total coke in the desilicated hydrocarbons is very low and is around 6.83%wt., and this is approximately 54 percent less than the amount of total coke in the fresh hydrocarbons (i.e., 12.62 wt.%). This low concentration of coke suggests high resistance to deactivation [54].

In fact, this percentage of coke accumulating on the surface of the laboratory-prepared catalyst is lower than the values reported in the literature, which range from 15 to 20 percent by weight of unmodified fresh Y-zeolites. The soft coke content was found to be 2.91 wt.%, indicating a small amount of reactive intermediates, while the hard coke content reached 3.92 wt.%, representing only about 57.4% of the total precipitated coke, compared to 72.5% in fresh HY catalyst. This suggests the presence of condensation of non-volatile hydrocarbon compounds, such as aromatics, due to the increased concentration of strong acids on the surface of the parent catalyst. Furthermore, the presence of intermediate coke (8.86 wt.%) and hard coke (5.77 wt.%) on the surface of the dealuminated HY catalyst indicates the retention and condensation of intermediates during the reaction. This prevents the rapid removal of the intermediate hydrocarbons formed in the hierarchical mesoporous, leading to blockage and/or deactivation of acid sites and thus the occurrence of coke-generating secondary reactions [9, 55]. In other words, this side reaction leading to coke formation occurs through the accumulation, buildup and subsequent polymerization of these intermediate hydrocarbons.

***Table 4. Coke deposition on spent catalysts.***

| Sample | Soft (wt.%) | Hard (wt.%) | Total (wt.%) |
|---|---|---|---|
| Fresh HY | 3.47 | 9.15 | 12.62 |
| Dealuminated | 3.09 | 5.77 | 8.86 |
| Desilicated | 2.91 | 3.92 | 6.83 |

Additionally, CHNS analysis provides crucial data for understanding the composition, purity, and origin of materials. It is an analysis for detecting the elements such as carbon (C), hydrogen (H), nitrogen (N), and sulfur (S), and sometimes oxygen (O), in both organic and inorganic samples. This is achieved by burning the samples at high temperatures to produce gases, which are then separated and analyzed. In fact, the CHNS analysis results confirm the TGA analysis findings, as both acid- and base-modified samples demonstrated an increased hydrogen-to-carbon ratio (i.e., H/C mass ratio) compared to the as-synthesized Y-sample, as shown in Table 5. This indicates that the parent HY-zeolite sample tends to form a graphite-like coke on its surface.

On the other hand, the modified samples show that coke is either less polycyclic aromatic compounds (i.e., less polyaromatic coke) on the surface of the dealuminated HY-zeolite sample, or hydrogen-deficient coke within the desilicated HY-zeolite sample. These results are consistent with the published literature [55].

***Table 5: Results of CHNS analysis of laboratory-prepared zeolite catalyst samples.***

| Zeolite | %H (wt. %) | %C (wt. %) | H/C mass ratio |
|---|---|---|---|
| HY | 3.0 ± 0.07 | 8.1 ± 0.14 | 0.37 ± 0.21 |
| Dealuminated HY | 3.2 ± 0.14 | 5.6 ± 0.07 | 0.57 ± 0.14 |
| Desilicated HY | 3.6 ± 0.07 | 4.8 ± 0.21 | 0.75 ± 0.07 |

### *3.2 Catalytic Performance Studies: Reaction Parameter Optimization*

The alkylation of toluene using 1-octene on the surface of each of the three zeolite catalysts was the subject of a systematic catalytic investigation in this study. The experiments were carried out in a multi-milliliter, encapsulated batch reactor. Mechanical stirring and continuous control of temperature and constant atmospheric pressure were employed. The reactions were conducted under a defined range of conditions to determine the optimal parameters and understand the reaction mechanisms to obtain the highest possible yield of the desired and industrially important products. Since alkylated toluene are valuable raw materials for surfactants, detergents, and specialty compounds, the alkylation of toluene is of great industrial importance [56]. Due to their selective pore size (i.e., micropores on the order of 7.4 Å) and their ability to catalyze alkylation processes effectively [57], HY-zeolites are among the most desirable catalysts and were therefore chosen in this study for the alkylation reactions [2].

#### 3.2.1 Time on Stream (TOS): Activity Development and Catalyst Deactivation

Alkylation reactions were carried out under selected standard conditions according to the experimental work (i.e., toluene to octene ratio 10:1, temperature 110 °C, and 350 mg of catalyst) over time periods ranging from 0 to 300 minutes to study the relationship between time on stream and the catalytic activity of the catalysts, as represented by the conversion . Significant differences in the activity patterns of the three catalysts were observed, as shown in Figure 9. This indicates the substantial influence of the structural modification (i.e., post-synthesis modification) of the parent catalyst through destructive methods (i.e., successive acid and/or base treatments) following its preparation from its

raw materials in the laboratory. The Fresh HY catalyst exhibited rapid initial activity, with conversion approaching 65% and exceeding around 85.5% after 30 and 300 min., respectively. It was also noted that the catalyst's activity stabilized after half the reaction time (i.e., 150 min.). This pattern of catalytic deactivation due to carbonaceous matter (i.e., either polyaromatic heavy coke or non-polyaromatic light coke) accumulation within the catalyst's pores (i.e., by either pore blockage or site coverage) is satisfactorily consistent with the findings in the literature [11].

Moreover, in dealuminated HY sample, the reaction rate is much slower, falling below 50% after 30 minutes and reaching 70% after 300 minutes. This is attributed to the reduced number of acid sites resulting from the removal of the aluminum to which the proton ($H^+$) is attached from the catalyst framework structure. In the case of desilicated HY, on the other hand, the sample exhibits excellent and high performance, with reaction rates exceedingly more than 70% and more than 90% after 30 and 300 minutes, respectively, and maintaining a stable rate of 90-92% after 150 minutes of alkylation time.

This remarkable stability, i.e., the decrease or delay in the rate of catalyst deactivation, is attributed to the hierarchical mesopores created within the catalyst framework structure as a result of the alkaline treatment by removing part of the silicon atoms, which made it able to avoid either pores blockage nor acidic sites deactivation, which made there a rapid removal of the hydrocarbon intermediates (i.e., polymerized hydrocarbons, which are the nuclei of the deactivated coke) formed during alkylation, which is consistent with the published literature [14]. Therefore, the desilicated HY-catalyst remains active for a longer period during the reaction compared to the other catalysts used in this study.

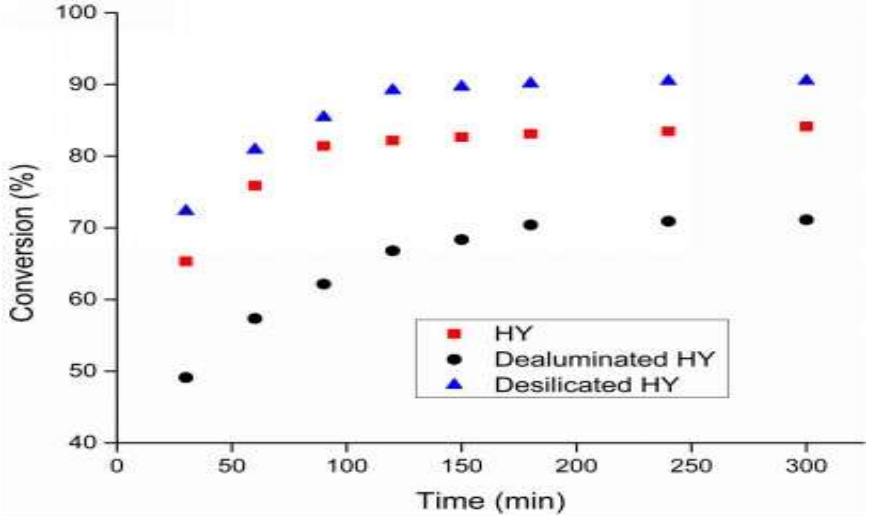



***Figure 9. Effect of time on stream on 1-octene conversion.***

### *3.2.2 Toluene:1-Octene Molar Ratio: Equilibrium and Transalkylation*

To investigate the effects of equilibrium and transalkylation throughout the reaction, the molar ratio of octene to toluene was adjusted to 1:4, 1:7, and 1:10, while the other alkylation conditions were kept constant at 110 °C, 350 mg of fresh HY catalyst, and 180 minutes. Figure 10 illustrates the potential for significantly improved conversion, increasing from below 40% at a 1:4 ratio to over 85% at a 1:10 ratio more than doubling the conversion rate.

The system can be said to reach equilibrium at a 1:10 ratio, where the reaction products are divided into monoalkylation products (2-, 3-, and 4-octyltoluene) and isomerization products (2-, 3-, and 4-octene), in addition to residues (i.e., coke species). The highest conversion to 2-octyltoluene, the primary target product of the reaction, is achieved at a molar ratio of 1:10 for octene to toluene. Only a slight shift towards isomerization

products is observed, while the shift is predominantly towards alkyl products, and small amounts of polyalkylation byproducts are also produced. When an excess of toluene is used (i.e., 1:10), the equilibrium is forced forward and allows the transalkylation of bulky polyalkylated products (i.e., bi- and tri-octyltoluenes) to monoalkylated products (i.e., mono-octyltoluenes) [9].

In general, it is observed that selectivity towards monoalkylation products increases at the expense of selectivity towards isomerization products as the toluene ratio in the reaction environment increases. In fact, the Y-zeolite pore structure is influencing the Ortho-selectivity and the access to the Meta and Para locations is restricted [5]. This is consistent with findings from published studies indicating that an excess of toluene can enhance conversion and selectivity and prevent the formation of precursors resulting from octyltoluene being trapped inside the zeolite's pore [49]. Based on the above, a 1:10 ratio of 1-octene: toluene provides optimal experimental conditions by balancing conversion and selectivity and obtaining the highest economically beneficial quantity of the 2-octyltoluene product.

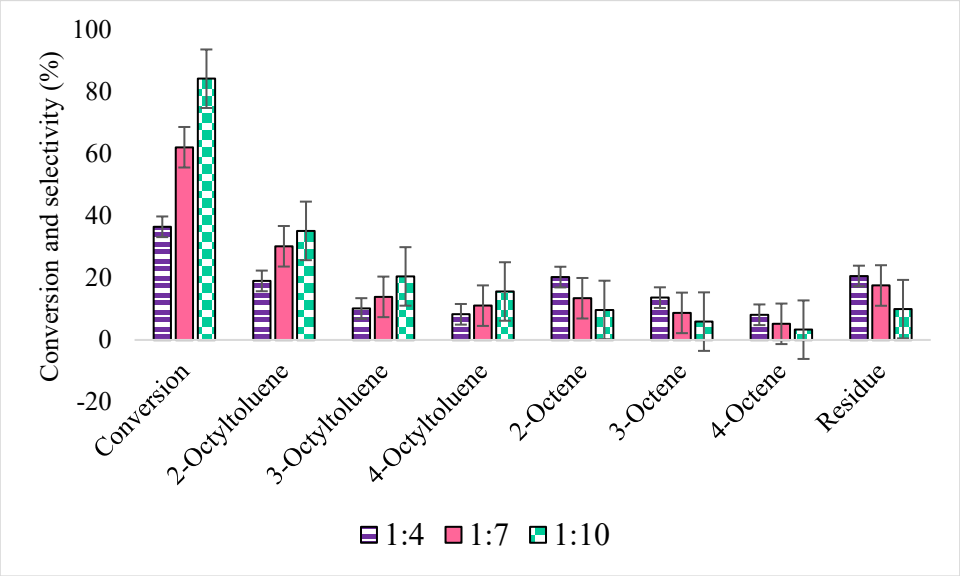



***Figure 10. Effect of toluene: 1-octene molar ratio on conversion and selectivity.***

### *3.2.3 Temperature Effect: Product Distribution*

Temperature plays a crucial role in the alkylation of toluene with 1-octene. Figure 11 illustrates the conversion of 1-octene, the selectivity of mono-octyltoluene and octene isomers as a function of temperature in the presence of HY parent catalyst. The effects of temperature between 90 and 110 °C were studied, with other reaction conditions held constant (i.e., 1:10 octene-toluene ratio, 350 mg of fresh HY, and 180 min). It was found that the conversion increased from 68.5% at 90 °C to 80.1% at 100 °C and then to 85.5% at 110 °C, representing a relative increase of 17% from the lowest to the highest temperature. This increase is logically consistent with published findings on this topic [64]. In general, the conversion increases with increasing temperature. After three hours, the selectivity for 2-octyltoluene production also increases with temperature (i.e., from 19% at 90 °C to 39% at 110 °C). Conversely, a decrease in the distribution of secondary octene isomers (i.e., 2-, 3-, and 4-octene isomers) is observed with increasing temperature from 90 to 110 °C. For example, the 2-octene isomerization reduced from 22% at 110 °C to 7.7% at 90 °C on the HY zeolite catalyst surface, as the distribution of isomerization reaction products is the opposite to that of alkylation reaction products [58]. The optimal temperature of 110 °C achieves a balance between highest conversion and appropriate

selectivity. According to previous conducted research, the optimal temperatures for alkylation on the HY zeolite surface are located somewhere in the range of over 90 °C to under 120 °C [8].

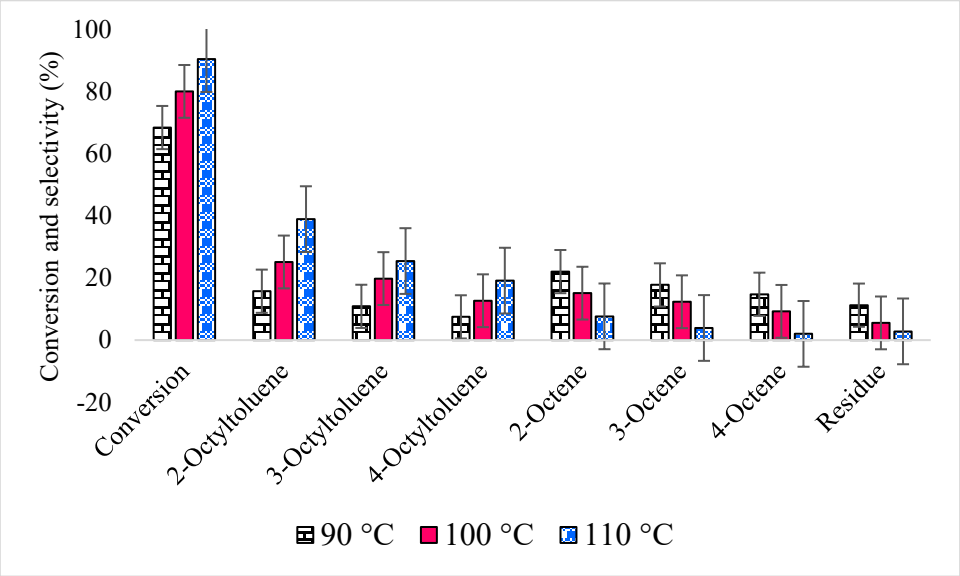



***Figure 11. Effect of reaction temperature on conversion and selectivity.***

### *3.2.4 Catalyst Amount: Active Site Density*

The dependence of the 1-octene conversion reaction on the amount of catalyst was studied and ranged from 150 to 350 mg using HY zeolite as a catalyst, while other reaction conditions remained constant (i.e. ratio 1:10, temperature 110 °C and duration 180 minutes). These experiments were primarily conducted to determine the dependence of alkylation reaction products on the catalyst's active site. Increasing the amount of catalyst increases the number of available active sites during the reaction, as it provides a larger surface area for the conversion of reactants to products, since catalysts are fundamentally interface phenomena. A steady increase in the conversion was observed over the specified time intervals, proportional to the increasing amount of catalyst used in the reaction, as shown in Figure 12. This conversion reached 78% with 150 mg, then 81% with 250 mg, and finally 85.5% with 350 mg of catalyst. The selectivity of the product distribution on the catalyst surface is predetermined by the natural selectivity of the pore geometry, leading to the formation of more carbonium ions per unit time, which directly increases the reaction rate [5]. The selectivity of 2-octyltoluene fluctuates between 20% and 40% of the total selectivity. According to previous studies, the alkylation rate on the zeolite surface is kinetically controlled and depends on the amount of catalyst used [2]. In fact, the composition of isomer within the products remains with higher selectivity for 2-isomer (i.e., 2-octene) compared to the other resulting isomers, as micropore structure provides continuous stereo-selectivity and does not depend solely on the density of acid sites.

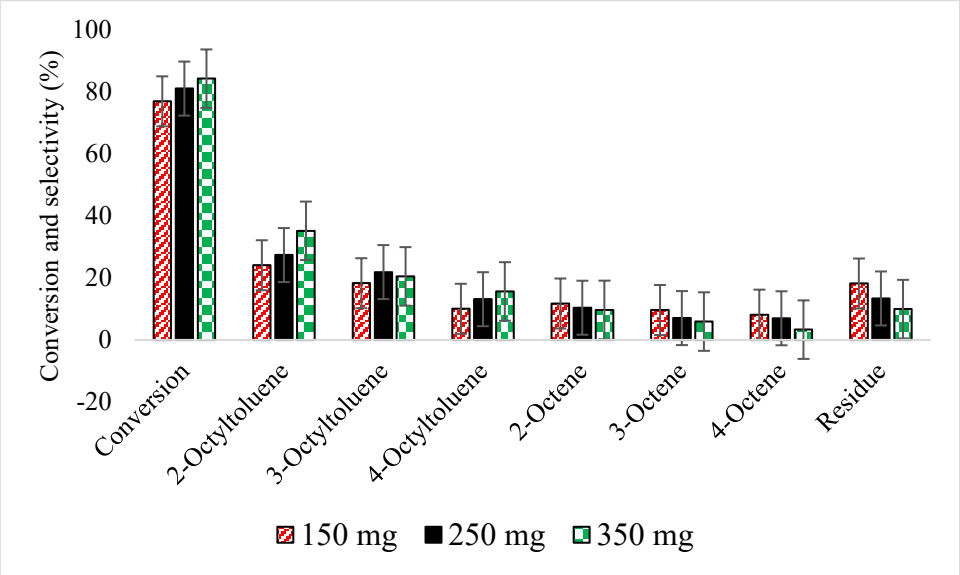



***Figure 12. Effect of catalyst amount on conversion and selectivity.***

### *3.3 The Relationship between the Physical Properties of a Catalyst and Its Catalytic Performance during Reactions*

#### *3.3.1 Dealuminated verses Fresh HY: Why Dealumination Fails?*

It is observed through the results of the experimental reactions carried out in the laboratory that the catalytic behavior of the dealuminated HY catalyst led to a decrease in the conversion on its surface to only 70%, compared to a conversion value of 85.5% on the surface of the parent HY zeolite catalyst. This significant decrease in performance is attributed to the removal of aluminum atoms and, consequently, the protons that represent strong Brønsted acids from its framework structure. This greatly affected the mechanism of catalyzing the alkylation process of the reactants on its surface. The increase in the silicon-to-aluminum ratio, which reached 5.3 compared to 4.5 within the lattice of the parent HY zeolite catalyst, is unquestionable proof of the loss of aluminum atoms, according to the published literature, acid treatment often causes a decrease in the catalytic activity of sensitive or complex reactions [36]. The liquid-phase toluene alkylation reaction with 1-octene is a complex, reversible heterogeneous reaction and is also a highly exothermic process, meaning it releases heat into the surroundings due to the simultaneous and competitive occurrence of alkylation, isomerization, and coke formation. Furthermore, the removal of aluminum atoms resulted in partial structural distortion of the catalyst, as revealed by X-ray diffraction pattern analysis. This led to a decrease in its crystallinity due to unit cell shrinkage caused by acid treatment, which could negatively impact its catalytic activity in such sensitive reactions. Furthermore, the dealuminated HY sample exhibits reduced textural characteristics, resulting in a surface area of 538.8 $m^2/g$ compared to 687.6 $m^2/g$ for the parent HY zeolite (Figure 13). This confirms the X-ray diffraction results, indicating partial structural collapse with a shrinkage of its unit cell (i.e., a smallest repeating unit chosen under certain rules to represent all the characteristics of a lattice.), resulting in a decrease in pore volume to 0.309 $cm^3/g$, compared to 0.337 $cm^3/g$ for the parent HY zeolite. Since alkylation reactions with relatively large reactant molecules require large pore sizes within the catalyst structure to form the desired alkylation products, the smaller pore size reduces the conversion of the desired alkylation products. Despite the reduced conversion, the positive aspect of acid treatment lies in minimizing the amount of coke accumulated within catalyst structure. This helps extend its service life in industrial processes. A

decrease in coke deposits to 8.86 wt.% is observed, compared to 12.62 wt.% for parent HY zeolite. This is attributed to the lower levels of strong acids within its structure. In fact, these acids accelerate the reaction and are the primary source of coke deposits from the intermediate materials formed, especially in narrow pore sizes. Therefore, the structural design of the catalyst used in alkylation reactions must be carefully selected to achieve the highest possible conversion and the lowest amount of coke deposits. The catalyst's long-term operational capability and reliability must also be considered to ensure the overall production process is economically viable [59].

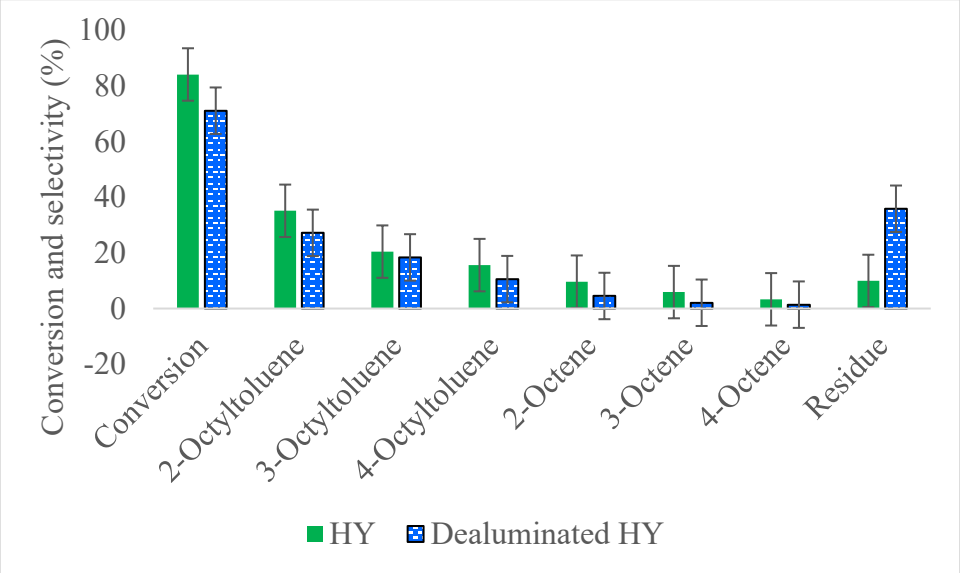



***Figure 13. Comparative performance of fresh HY verses dealuminated HY.***

### *3.3.2 Desilicated vs. Fresh HY: Advantages of Hierarchical Structure*

The experimental results show that the desilicated HY catalyst exhibited superior catalytic behavior compared to the parent HY zeolite catalyst. As previously mentioned, the conversion peaked on its surface, reaching approximately 92%, compared to 85.5% on the fresh HY catalyst surface. This occurred despite a significant decrease in coke deposition within its structure, reaching approximately half (6.83 wt.%), compared to the 12.62 wt.% of coke accumulated within the parent HY zeolite framework

Although the strong acidic sites associated with aluminum atoms within the desilicated HY catalyst were not significantly affected by the removal of silicon atoms, coke deposition remained low on its surface. This supports the conclusion that the arrangement and increased density of the acidic sites (lower Si/Al ratio: 4.0 versus 4.5 for the parent HY) resulted in a more ordered reaction rate, accelerating the transformation of the intermediate compounds formed within its pores without allowing for higher coke deposition.

In other words, the base treatment contributed to increased catalytic efficiency of the catalyst, and yielded a significant difference, which resulted in greater catalyst stability and a longer lifespan. X-ray diffraction patterns of the desilicated HY catalyst reveal an increased degree of crystallinity due to the heightened intensity of its peaks. The base treatment likely helped remove impurities from its structural framework and logically led to structural opening via removing silicon atoms, considering that silicon is the basis of tetrahedrons within zeolite lattice.

This resulted in an expansion of the unit cell. It's worth noting that tetrahedrons are called primary-building units (PBUs) and combine to form secondary-building units, or SBUs, which give rise to the unique topology. The higher values obtained from the textural

characteristics analysis of the desilicated HY sample compared to the fresh HY sample confirm a significant expansion in its structural composition. The surface area of the desilicated HY catalyst was 700.5 $m^2/g$ compared to 687.6 $m^2/g$ for the fresh HY catalyst, and the average pore volume was larger at 0.344 $cm^3/g$ compared to 0.337 $cm^3/g$ for the fresh HY catalyst (Figure 14).

Furthermore, the significant reduction in coke formation on the surface of the desilicated HY catalyst, along with the increased conversion compared to the catalytic behavior of the parent HY catalyst, indicates that the hierarchical intermediate mesoporosity prevents the deactivation of acidic sites by enabling rapid product removal and inhibiting its polymerization. Meanwhile, the retention of intermediate compounds within the relatively small, finely microporous of fresh HY structure increases the likelihood of blocking acidic sites and thus the formation of hard coke (i.e., highly concentrated aromatic compounds).

This aligns with the scientific literature on hierarchical mesoporosity of zeolites [60]. Extending the catalyst lifetime in macromolecular reactions such as alkylation by dramatically reducing the amount of coke deposited on its surface is a key focus of current research. The present work provides strong experimental evidence that silica removal is preferable to aluminum removal for modifying zeolite structures in challenging catalytic applications. Recent studies also increasingly point to the need for hierarchical zeolites in next-generation catalysts [61, 62].

Finally, To interpret the results obtained from this study in light of the mechanisms of alkylation reactions described in the published literature, and to gain a deeper understanding of the performance of zeolite catalysts, the reaction pathways revealed that the steps involved in the carbonium mediation of toluene alkylation include: (1) carbonium formation via the protonation of 1-octene ($CH_2CHC_6H_{13}$) at Brønsted acid sites (Si-OH-Al); (2) carbonium attack on the toluene aromatic ring ($C_6H_5CH_3$) within the hierarchical mesopores, resulting in alkyl formation with a regenerated acid site; (3) adsorption of the product; and (4) transalkylation of the product with toluene to obtain a desired product such as 2-octyltoluenes.

Due to the 7.4 Å pore structure of fresh HY zeolite, access to aromatic sites is limited, meaning that ortho-substitution and mono-alkylation processes are more advantageous than poly-alkylation procedures. Deactivation occurs due to the accumulation of intermediate reactants.

Large polyalkylation molecules move slowly over structures with relatively narrow micropores and remain in contact with acidic sites long enough to form hard coke through further condensation reactions. On the other hand, the hierarchical mesopores, as within the desilicated HY zeolite, overcome these limitations by providing rapid diffusion channels for the bulky intermediate molecules.

Consequently, desilicated HY catalyst exhibits a lower hard coke content of approximately 3.92 wt.% compared to the high percentage deposited on the surface of fresh HY catalyst, which reaches 9.15 wt.%. Furthermore, desilicated HY catalyst remains active with a stable conversion that increases to over 90% within just 150 minutes, providing direct evidence of its mass-transfer improvement. These findings are strongly supported by hierarchical catalyst design concepts that are consistent with what is known in the scientific literature about the mechanisms underlying zeolite deactivation [63].

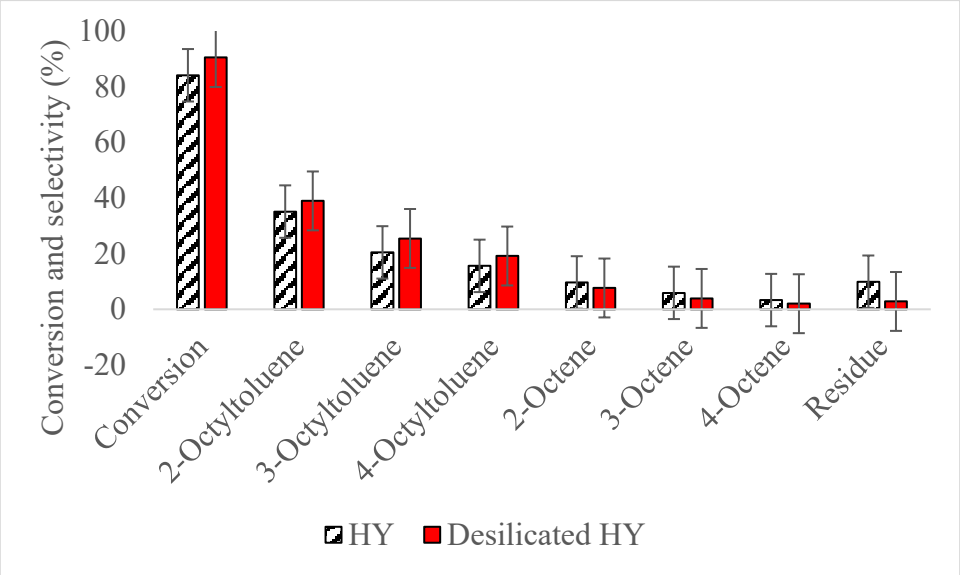



***Figure 14. Comparative performance of fresh HY verses desilicated HY.***

### *4. Conclusions*

This paper showed the approach employed to adjust the HY zeolite structure is absolutely critical to catalytic performance and avoidance of coke formation during liquid-phase toluene alkylation with bulky olefinic substances. Desilicated HY was found to be the most active and stable compared to the rest of the catalysts investigated and this is directly related to the formation of hierarchical mesoporosity, which increases the intracrystalline diffusion and decreases secondary condensation reactions that cause deactivation of the catalyst. Conversely, dealumination decreased the catalytic activity and coke generation by decreasing the Brønsted acidity and partly damaging the structure of the framework, which restricted the accessibility of large molecules to the active site. Coke analyses by elements revealed that the better pathways of diffusion prefer the creation of less condensed species of carbon. Comprehensively, these findings demonstrate clearly that the hierarchical porosity formation through controlled desilication is a superior and stronger method compared to acidity reduction in alleviating catalyst deactivation in aromatic alkylation reactions that involve large olefins, making desilicated HY zeolite a potentially useful design of catalysts in industry.

### *References*

1. Sohn, S. and P. Do, Linear Alkylbenzenes: An Overview of the Commercial HF and Detal™ Process Unit Alkylation Technology (Case Study), in Industrial Arene Chemistry. 2023. p. 729-745.
2. Al-Sultani, S.H., et al., Sustainable Liquid-Phase Alkylation of Toluene Using Zeolitic Catalysts: A Comparative Evaluation of Al-Rich Y and Si-Rich Beta Zeolites for Industrial Green Chemistry to Support Sustainable Development Goals (SDGs). 2025. 6(2): p. 24 %J ASEAN Journal of Science and Engineering.
3. Rueping, M. and B.J. Nachtsheim, A review of new developments in the Friedel–Crafts alkylation – From green chemistry to asymmetric catalysis. Beilstein Journal of Organic Chemistry, 2010. 6.
4. Pan, A., et al., Synergistic Brønsted/Lewis acid catalyzed aromatic alkylation with unactivated tertiary alcohols or di-tert-butylperoxide to synthesize quaternary carbon centers. Chemical Science, 2022. 13(12): p. 3539-3548.

5. Al-Sultani, S.H., A. Al-Shathr, and B.Y. Al-Zaidi, Toluene Alkylation Reactions over Y-Type Zeolite Catalysts: An Experimental and Kinetic Study. 2024. 5(4): p. 1042-1065.
6. Armor, J.N., A history of industrial catalysis. Catalysis Today, 2011. 163(1): p. 3-9.
7. Khalil, M., et al., Experimental and Kinetic Study of the Catalytic Behavior of Sulfate-Treated Nanostructured Bifunctional Zirconium Oxide Catalysts in n-Heptane Hydroisomerization Reactions. 2023. 7(6): p. 115.
8. Al-Sultani, S.H., A. Al-Shathr, and B.Y. Al-Zaidi, Aromatics Alkylated with Olefins Utilizing Zeolites as Heterogeneous Catalysts: A Review. 2024. 5(4): p. 900-927.
9. Guisnet, M., "Coke" molecules trapped in the micropores of zeolites as active species in hydrocarbon transformations. Journal of Molecular Catalysis A: Chemical, 2002. 182–183: p. 367-382.
10. Chen, F.-J. and J. Yu, Discovery of Stable Extra-large Pore Zeolites Based on Rational Design of Structure-directing Agents. Accounts of Chemical Research, 2025. 58(15): p. 2402-2414.
11. Al-Shathr, A., et al., Experimental and kinetic studies of the advantages of coke accumulation over Beta and Mordenite catalysts according to the pore mouth catalysis hypothesis. Catalysis Communications, 2023. 181: p. 106718.
12. Waqas, M., et al., Mesostructured bimetallic MFI zeolite for efficient aromatization of light naphtha to BTX aromatics. Journal of Porous Materials, 2025.
13. Quintana-Gómez, L., et al., "Reverse combustion" of carbon dioxide in water: The influence of reaction conditions. Frontiers in Energy Research, 2022. 10: p. 917943.
14. Al-Shathr, A., et al., Investigation of toluene alkylation with hept-1-ene over fresh and modified h-beta catalysts according to apparent activation energy values. South African Journal of Chemical Engineering, 2025. 54: p. 114-132.
15. Roth, W.J., et al., Top-down engineering of zeolite porosity. Chemical Society Reviews, 2025. 54(16): p. 7484-7560.
16. Hijazi, N., et al., Chemical engineering of zeolites: alleviating transport limitations through hierarchical design and shaping. Chemical Society Reviews, 2025. 54(13): p. 6335-6384.
17. Guo, X., et al., Enhancing Atomic Layer Deposition Efficiency of the Classical Medium-Pore ZSM-5 Zeolite by an Artful Alkali-Etching Technique for Boosting NH3-SCR Behaviors. Environmental Science & Technology, 2026. 60(2): p. 2245-2254.
18. Miyashita, K., et al., Quantitative Estimation of Effective Brønsted Acid Sites of Silica-Supported H4SiW12O40 Heteropoly Acid for Adsorption of Various Molecules. Langmuir, 2025. 41(2): p. 1491-1501.
19. Corma, A., From Microporous to Mesoporous Molecular Sieve Materials and Their Use in Catalysis. Chemical Reviews, 1997. 97(6): p. 2373-2420.
20. Cui, J.-W., et al., Engineering Hierarchy to Porous Organic Cages for Biomimetic Catalytic Applications. Accounts of Materials Research, 2025. 6(4): p. 484-498.
21. Patra, K., et al., Harnessing Advanced Porous Materials, Covalent Organic Frameworks, and Porous Organic Polymers as Next-Generation Porous Frameworks for Targeted Removal of Emerging Water Contaminants. ACS Applied Engineering Materials, 2025. 3(5): p. 1130-1165.
22. Wang, H., Q. Wu, and F.-S. Xiao, Design of zeolite-based catalysts by Le Chatelier's principle. Applied Catalysis B: Environment and Energy, 2025. 379: p. 125671.
23. Zhu, Z., et al., The roles of acidity and structure of zeolite for catalyzing toluene alkylation with methanol to xylene. Microporous and Mesoporous Materials, 2006. 88(1): p. 16-21.

24. Degnan, T.F., Applications of zeolites in petroleum refining. Topics in Catalysis, 2000. 13(4): p. 349-356.
25. Guisnet, M., L. Costa, and F.R. Ribeiro, Prevention of zeolite deactivation by coking. Journal of Molecular Catalysis A: Chemical, 2009. 305(1–2): p. 69-83.
26. Tao, Y., et al., Mesopore-Modified Zeolites: Preparation, Characterization, and Applications. Chemical Reviews, 2006. 106(3): p. 896-910.
27. Jiang, J., J. Yu, and A. Corma, Extra-Large-Pore Zeolites: Bridging the Gap between Micro and Mesoporous Structures. 2010. 49(18): p. 3120-3145.
28. Derouane, E.G., et al., The Acidity of Zeolites: Concepts, Measurements and Relation to Catalysis: A Review on Experimental and Theoretical Methods for the Study of Zeolite Acidity. Catalysis Reviews, 2013. 55(4): p. 454-515.
29. Blatter, F. and E. Schumacher, The preparation of pure zeolite NaY and its conversion to high-silica faujasite: An experiment for laboratory courses in inorganic chemistry. Journal of Chemical Education, 1990. 67(6): p. 519.
30. Martínez, C. and A. Corma, Inorganic molecular sieves: Preparation, modification and industrial application in catalytic processes. Coordination Chemistry Reviews, 2011. 255(13): p. 1558-1580.
31. Pérez-Ramírez, J., et al., Hierarchical zeolites: enhanced utilisation of microporous crystals in catalysis by advances in materials design. Chemical Society Reviews, 2008. 37(11): p. 2530-2542.
32. Zhu, T., et al. Synthesis and Applications of Zeolite-Encapsulated Metal Catalysts. Catalysts, 2025. 15, DOI: 10.3390/catal15090836.
33. Kim, D.W., D.S. Choi, and J.B. Joo, Synthesis of hierarchical zeolites for enhanced catalytic cracking performance toward larger hydrocarbon molecules. Advances in Industrial and Engineering Chemistry, 2025. 1(1): p. 30.
34. Serrano, D.P., J.M. Escola, and P. Pizarro, Synthesis strategies in the search for hierarchical zeolites. Chemical Society Reviews, 2013. 42(9): p. 4004-4035.
35. Svelle, S., et al., How defects and crystal morphology control the effects of desilication. Catalysis Today, 2011. 168(1): p. 38-47.
36. Wei, Y., et al. Tailoring and visualizing the pore architecture of hierarchical zeolites. 2015. DOI: 10.1039/C5CS00155B.
37. Martins, A., et al., Zeolites and Related Materials as Catalyst Supports for Hydrocarbon Oxidation Reactions. 2022. 12(2): p. 154.
38. Maschmeyer, T. and L. van de Water, An Overview of Zeolite, Zeotype and Mesoporous Solids Chemistry: Design, Synthesis and Catalytic Properties, in Catalysts for Fine Chemical Synthesis. 2006. p. 1-38.
39. Groen, J.C., Mesoporous Zeolites Obtained by Desilication. 2007, Netherlands: Ponsen & Looijen B.V.
40. Dědeček, J., Z. Sobalík, and B. Wichterlová, Siting and Distribution of Framework Aluminium Atoms in Silicon-Rich Zeolites and Impact on Catalysis. Catalysis Reviews, 2012. 54(2): p. 135-223.
41. Lutz, W. Zeolite Y: Synthesis, Modification, and Properties—A Case Revisited. Hindawi Publishing Corporation 2014 [cited 2014; 1-20]. Available from: http://www.hindawi.com/journals/amse/2014/724248/
42. Groen, J.C., et al., Mechanism of hierarchical porosity development in MFI zeolites by desilication: the role of aluminium as a pore-directing agent. Chemistry, 2005. 11(17): p. 4983-94.
43. Bian, Y., et al., Nanosheet zeolites: controlled synthesis, characterization, and advanced catalysis applications. Materials Horizons, 2025. 12(18): p. 7133-7159.

44. Lee, H., et al., Unveiling the Catalytic Superiority of Ti-MWW Zeolite for Sustainable Lactide Production from Methyl Lactate. ACS Omega, 2025. 10(50): p. 62134-62144.
45. Sarkar, S., et al., The multifaceted role of zeolites in modern agriculture and environmental management. Journal of Plant Nutrition, 2025. 48(20): p. 3589-3616.
46. Verboekend, D. and J. Pérez-Ramírez, Design of hierarchical zeolite catalysts by desilication. Catalysis Science & Technology, 2011. 1: p. 841-1084.
47. Silaghi, M.-C., C. Chizallet, and P. Raybaud, Challenges on molecular aspects of dealumination and desilication of zeolites. Microporous and Mesoporous Materials, 2014. 191: p. 82-96.
48. Talebian-Kiakalaieh, A. and S. Tarighi, Synthesis of hierarchical Y and ZSM-5 zeolites using post-treatment approach to maximize catalytic cracking performance. Journal of Industrial and Engineering Chemistry, 2020. 88: p. 167-177.
49. Da, Z., P. Magnoux, and M. Guisnet, Liquid phase alkylation of toluene with 1-heptene over a HFAU zeolite: evidence for transalkylation between toluene and non-desorbed products. Applied Catalysis A: General, 1999. 182(2): p. 407-411.
50. Čejka, J. and B. Wichterlová, ACID-CATALYZED SYNTHESIS OF MONO- AND DIALKYL BENZENES OVER ZEOLITES: ACTIVE SITES, ZEOLITE TOPOLOGY, AND REACTION MECHANISMS. Catalysis Reviews, 2002. 44(3): p. 375-421.
51. Ponomareva, O.A., et al., Benzene alkylation with dodecene-1 over micro-mesoporous molecular sieves. Petroleum Chemistry, 2010. 50(6): p. 427-436.
52. Kim, M.-R. and S. Kim, Enhanced Catalytic Oxidation of Toluene over Hierarchical Pt/Y Zeolite. 2022. 12(6): p. 622.
53. Ahmed, R., C.M. Sinnathambi, and D. Subbarao, Kinetics of De-coking of Spent Reforming Catalyst. Journal of Applied Sciences, 2011. 11: p. 1225-1230.
54. Bauer, F. and H.G. Karge, Characterization of Coke on Zeolites, in Characterization II, H.G. Karge and J. Weitkamp, Editors. 2007, Springer Berlin Heidelberg: Berlin, Heidelberg. p. 249-364.
55. Cerqueira, H.S., et al., Coke formation and coke profiles during the transformation of various reactants at 450°C over a USHY zeolite. Applied Catalysis A: General, 2001. 208(1): p. 359-367.
56. Dong, H.-j. and L. Shi, Alkylation of Toluene with t-Butyl Alcohol over Zeolite Catalysts. Industrial & Engineering Chemistry Research, 2010. 49(5): p. 2091-2095.
57. Ma, H., et al., Metal-Modified Zeolites for Catalytic Dehydration of Bioethanol to Ethylene: Mechanisms, Preparation, and Performance. 2025. 15(8): p. 791.
58. Magnoux, P., et al., Influence of the acidity and of the pore structure of zeolites on the alkylation of toluene by 1-heptene, in Studies in Surface Science and Catalysis, A.B. H.U. Blaser and R. Prins, Editors. 1997, Elsevier. p. 107-114.
59. Lovás, P., et al., Preparation of an active and regenerable catalyst for liquid-phase alkylation of toluene with 1-decene. Applied Catalysis A: General, 2014. 475: p. 341-346.
60. Pérez-Pariente, J., M. Sanchez-Sanchez, and J. Pliego, Post-Synthesis Surfactant-Induced Mesoporosity in Zeolite Crystals: State-of-the-Art, Open Questions and Perspectives. 2025. p. 315-358.
61. Rutkowska, M. and L. Chmielarz, Application of Mesoporous/Hierarchical Zeolites as Catalysts for the Conversion of Nitrogen Pollutants: A Review. 2024. 14(5): p. 290.

62. Bekele, B.T. and R. Gounder, Extra-Framework Aluminum Moieties Occluded within Zeolite Micropores Strengthen Dispersive Stabilization of Confined Alkanes and Carbocationic Transition States. ACS Catalysis, 2025. 15(24): p. 21100-21114.
63. Zhu, X., et al., Constructing Hierarchical Zeolites with Highly Complete Framework via Controlled Desilication. 2024. 63(50): p. e202411446.